OPTOELECTRONIC PROPERTIES OF

POLY(*P*-PHENYLENE VINYLENE)

FOR APPLICATION IN LIGHT EMITTING DEVICES

BY

MOHAMMAD ESTEGHAMATIAN, B.SC., M.A.SC.

A thesis

submitted to the School of Graduate Studies

in partial fulfillment of the requirements for the degree of

Doctor of Philosophy

McMaster University

OPTOELECTRONIC PROPERTIES OF POLY(*P*-PHENYLENE VINYLENE)

DOCTOR OF PHILOSOPHY (1995)   **MCMASTER UNIVERSITY**

(Materials Science and Engineering)   Hamilton, Ontario

TITLE: Optoelectronic Properties of Poly(p-phenylene vinylene)

For Application in Light Emitting Devices

AUTHOR: Mohammad Esteghamatian,   B.Sc.   (Shiraz University, Iran)

M.A.Sc (Windsor University, Canada)

SUPERVISOR: Professor Gu Xu

NUMBER OF PAGES: 150, xv

ii

ABSTRACT

Organic electroluminescent devices (OLED's) have been intensely researched in recent years. Poly(p-phenylene vinylene) (PPV), due to its ease of processing and potential high quantum yield, is considered a good candidate for future display applications. By synthesizing PPV films and fabricating PPV-based organic ELD's, optoelectronic properties of this conjugated polymer were investigated. The PPV synthesis was modified to improve material quality which affected device stability, lifetime, and luminescent yield.

By utilizing transmission electron microscopy, the presence of PPV crystals which lowered the quantum yield was thoroughly investigated. Electron micrographs revealed that aggregates of crystals were embedded in an amorphous matrix. Analysis of diffraction patterns established that NaCl was a major impurity and that its crystals acted as nucleation sites. Steps were accordingly taken to exclude NaCl and prepare a more amorphous material.

Impedance spectroscopy was used to measure conductivity and the activation energy. The low activation energy suggested carrier transport via

hopping between localized states. Furthermore, the presence of a metal/polymer interface, which limited charge injection into the sample and lowered the efficiency, was identified. By controlling the parameters affecting device/material preparation, this interface was to a great extent improved.

Electroluminescent devices with areas of 40 mm^2 were fabricated. These devices could draw currents of up to 0.2 mA/cm^2 and emit a yellowish green light, visible under laboratory lighting at various viewing angles. An external efficiency of 0.4 Lum/Watt was attained. A conservative internal efficiency of 0.59%, significantly higher than the ones previously reported for single layer organic devices, was calculated. The threshold voltage was reduced to 2-5 volts and stable OLED's with a lifetime of over 160 hours were fabricated.

The photovoltaic effect in PPV was explored by employing delayed-collection-field and field-induced fluorescent quenching techniques. A carrier generation efficiency of 42% was obtained. The strong field dependence of the carrier generation efficiency was noticed which supported the formation of bound electron-hole pairs.

ACKNOWLEDGEMENT

The author wishes to thank **Dr. Gu Xu** for his supervision, helpful discussions and constant guidance throughout the course of this work and for providing a positive and constructive environment for his research group.

The author wishes to express his gratitude to **Dr. Adrian Kitai** for his very important and useful discussions and hints, and for generously allowing us to use his laboratory and equipment, without which this research could have not been completed.

The author also wishes to thank **Dr. Harald Stover** for his help, guidance and hints throughout the PhD meetings.

And, last but not least, the author would like to thank the **polymer group** for their support and useful discussions.

Table of Contents

List of Figures

List of Tables

Chapter 1

Introduction

Light emitting devices are of great importance in everyday life. They cover a range of applications from television sets and computer monitors to wrist watches, digital displays and navigation instruments. In general, these devices can be classified into four categories; cathode ray tubes (CRT's), liquid crystals displays (LCD's), semiconductor light emitting diodes (LED's), and electroluminescent panels (EL's). CRT's, which currently represent a majority of the market share, have complicated structures and are bulky, thus not suitable for large area or portable display devices. Liquid crystal based devices, on the other hand, are becoming more popular and have applications from wrist watches to lap top computers to cockpit navigation instruments. Although they offer several advantages over CRT's including less weight and lower power consumption, LCD's suffer from three important drawbacks: small viewing angle (±45 degrees), limited temperature range (-20 to + 50 °C), and a need for a front or back illumination source. Another area of concern in LCD's is the high manufacturing cost. For example, an active matrix liquid

crystal display is made up of millions of pixels, each of which is controlled by

a transistor. Malfunctioning of only a few transistors results in poor display

quality and increases the percentage of rejects and, thus, the manufacturing

cost.

The third class of display devices consists of light emitting diodes

which are made of single crystals of inorganic semiconductor materials such

as group III-V elements (i.e. GaAs), or alloys of group II-VI and group III-V

elements (i.e. GaInPAs). These devices are usually fabricated in the form of

a p-n junction or multi-layers of p- and n-type semiconductor materials. Each

layer requires to be free of defects (dislocations and impurities) and have a

lattice parameter which closely matches the lattice parameter of the other

layers. The complicated process for achieving these requirements leads to a

high manufacturing cost and also limits the size of each device to about 6 by

6 square inches.

In the last category, a typical EL device is prepared by placing a doped

phosphor material between two insulating layers onto which two electrodes are

deposited. A high AC field is applied to the electrodes and while only a little

current is generated, a high potential is required to excite dopant atoms. Light is emitted upon relaxation of the atoms. Despite the ease with which one can tune the emitted colour in these inorganic materials (e.g. by controlling the composition or thickness), fabrication of defect-free and highly efficient devices having a long lifetime is quite difficult and challenging and is currently a subject of intense research.

Most recently, a new class of light emitting devices has been introduced which is based on conjugated organic materials. These organic light emitting display devices (OLED's) are prepared by placing suitable conducting and fluorescent polymers between two conducting electrodes (at least one transparent) which are connected to positive and negative poles of a low voltage DC power source. Injection of electrons into the conduction band and holes into the valence band of the polymer and subsequent electron-hole (e-h) recombination leads to light emission. In this study the fabrication, advantages and disadvantages of organic light emitting devices based on poly(p-phenylene vinylene) PPV, one of the most promising candidate for an OLED, are investigated.

1.1 Background and Literature Review

a) Energy Gap Formation and Conduction Mechanism

Traditionally polymers were known for their insulating properties and were mainly used as dielectrics and where electrical insulation was required. Discovery of conducting polyacetylene $(-CH=CH-)_n$ was indeed an important step in providing scientists with a new class of conducting materials. The accidental discovery of highly conducting polyacetylene films started the intense research on the mechanism of conduction in unsaturated polymers (see, for example, Shirikawa 1977, 1978, 1979/1980, and Narmaan 1977 and the references therein).

The intrinsic conductivity of polyacetylene measured at room temperature was reported as $\sigma=10^{-5}$ S/cm for the trans-isomer and $\sigma=10^{-9}$ S/cm for the cis-material (Chiang 1978). The conductivity of polyacetylene can be enhanced to $\sigma=10^5$ S/cm upon doping and/or stretch-orientation of the molecules. Considering its low density, conductivity to weight ration of polyacetylene exceeds most metallic conductors including copper (Narmaan 1987). The high conductivity in polyacetylene is attributed to the presence of loosely bound π-electrons which are delocalized along the conjugated

backbone and, therefore, charge transport in pure polyacetylene is essentially one dimensional. In heavily doped polyacetylene, however, carrier transport occurs in a disordered fashion via hopping mechanisms as will be discussed below.

Being a linear polymer and having a simple structure of alternating single and double carbon-carbon bonds, polyacetylene has been studied by researchers as a model to explain the carrier transport process in conjugated materials. When two carbon atoms form a double bond, each carbon atom with its four outer shell electrons undergoes hybridization by forming three sp^2 and one 2p orbitals. Two sp^2 orbitals, one from each atom, form a sigma bond with a dissociation energy of 95 KCal/mole, and the overlap of the 2p orbitals form a π bond with a dissociation energy of 67 KCal/mole (Atkins 1994), as schematically drawn in Fig. 1.1. Due to a lower dissociation energy, π electrons are more loosely bound to the nuclei and, therefore, can move more freely. Because of weak interchain coupling, delocalization of the π electrons occurs mainly along the polymeric chains and these systems are said to be electronically one dimensional (Ngai 1986 and Heeger 1988). The models used to explain the conducting process in polymers are mostly based on a

single chain one-electron model, where bond alternation (short and long bonds) is the key to the energy gap formation. In other words, if the bond lengths were all equal, delocalization would lead to each bond having equal partial double-bond character, energy bands would overlap and the polymer would behave like a quasi one dimensional metal. However, due to alternating single (long) and double (short) bonds, polyacetylene behaves like a semiconductor (Heeger 1988 and Aldissi 1989). This is summarized in Peierls distortion theorem (Cowie 1991), which states that bond alternation results in lattice distortion and consequently breaks the continuity of the energy bands and, thus, leads to the formation of a band gap, as depicted in Fig. 2.1. By varying the size of the band gap, a polymer can then become a conductor or an insulator.

Considering the wide range (10^{14}) in conductivity of polyacetylene, one mechanism can not explain charge transport over the entire range. For example, charge transport in pure polyacetylene is ascribed to the presence of chain defects. These defects are formed between two dimers of (e.g.) trans-polyacetylene as a result of a break in the continuity of the bond alternation pattern, and are called neutral solitons (Heeger 1988 and Cowie 1991). Since

polyacetylene is two-fold degenerate, i.e. the two dimers have equal energies, the motion of a soliton along a polymeric chain transforms one dimer into another, resulting in the transport of charge carriers along the chain. Upon doping, neutral solitons can be positively charged (p-type doping) or negatively charged (n-type doping), which can further enhance the conductivity. It should be noted that at low doping levels, polymer chains do not form bonds with the dopant atoms and charge transfer occurs from the dopant atoms to the polymer chains which act as polyanions or polycations. At high doping levels, however, there is an increased reaction of the dopants with the polymer chains leading to local disorder and to the formation of localized states, which can act as hopping sites for charge carriers.

Interchain hopping mechanism is also an important conduction process in disordered solids (Roth 1991). Hopping is a common mode of charge transport in non-degenerate ground state polymers such as poly(p-phenylene vinylene) ($-C_6H_6-CH=CH-)_n$. In these polymers, the motion of solitons is restricted, and the confined solitons (polarons) contribute to the conductivity by acting as hopping sites.

Although, conductivity of PPV has been measured by several investigators (Murase 1985 and Tokito 1986), little mention has been made of carrier transport process in PPV. In this study attempts are also made to shed some light on this process by determining temperature-dependence of conductivity and measuring current-voltage characteristics, as is discussed in Chapters 3 and 5.

b) Organic LED's and Mechanism of Electroluminescence

There are numerous conducting polymers but only some of them are capable of emitting visible light upon excitation. Regardless of the excitation source the colour (wavelength) of the emitted light is determined by the size of the energy gap. Polyacetylene, for example, has a band gap of $E_g=1.5$ eV, ($\lambda=830$ nm) (Werner 1995), which is almost out of the visible spectrum and thus not suitable for OLED's. However, the energy gap of conjugated polymers can be tuned by altering the molecular structure of the polymeric unit or modifying the conjugation length (Tang 1989, Burn 1992, Kido 1993, Yang 1993, Esteghamatian 1994-b, Beggren 1994, and Werner 1995). This important feature enables us to design a polymer with proper band gap which can emit light in the desired part of the visible spectrum. For example, by

combining acetylene and polyphenylene a fluorescent material (PPV) with

E_g=2.4 eV (516 nm) is obtained, which emits light in the yellow-green part of

the visible spectrum.

The optical properties of PPV attracted some attention only when it was

accidentally exposed to ultraviolet radiation and a greenish colour was

observed. The insolubility of PPV, however, posed as a major obstacle in

preparing thin films required for display applications. In this thesis a two-step

procedure known as precursor route is employed to obtain uniform and robust

films of PPV having thicknesses ranging from 30 nm to 5000 nm (Wessling

1972, Capistran 1984, Bradley 1987-a, Gagnon 1987, and Burroughes 1990).

Utilization and modification of this method, which will be discussed in detail

in Chapter 2, has provided the flexibility to easily fabricate electronic devices

and study their optoelectronic characteristics.

PPV-based OLED's are usually made by casting, spin coating of PPV

solution, or vacuum deposition of PPV onto a conductive substrate. The

sample is then placed in a vacuum furnace to eliminate unwanted side groups

from the main chains. The temperature and duration of the elimination process

play important roles in the final quality of the film. It has been reported that full conversion of PPV can be achieved at T≥320 °C (Bradley 1987-a and Gmeiner 1993). However, as will be demonstrated later in Chapter 4, with increasing the elimination temperature, the film quality and light intensity decrease and, therefore, lower temperatures are desirable for the elimination process. The presence of carbonyl groups in PPV, which becomes more significant with increasing elimination temperature, also greatly affects the lifetime and efficiency of OLED's and should be avoided. In the present work a study has been carried out to achieve full conversion at lower temperatures under a protective atmosphere rather than vacuum, thus improving polymer quality and enhancing device stability and lifetime.

Electroluminescence in PPV-based devices is produced by injection of electrons (e) and holes (h) from negative and positive electrodes into the polymer. Oppositely charged species, which are transported as polarons under an applied field, capture one another to form excitons (Friend 1992 and Antoniadis 1994). Radiative decay of these singlet excitons will then lead to luminescence. The formation of bound e-h pairs (excitons) as the primary excitation mode has been disputed by several investigators (Lee 1993 and

1994). However, the similarity between the EL and photoluminescence (PL)

spectra indicates that, regardless of the excitation source, the same excited

states are produced by charge injection as by photoexcitations (Friend 1992).

This observation and the fact that a high voltage (Esteghamatian 1995) is

required for e-h dissociation and for the collection of photogenerated charge

carriers are indicative of the formation of strongly correlated e-h pairs. (see

section 1.1.c and Chapter 3.IV. on photovoltaic measurements).

The low quantum efficiencies of these devices, 0.005% (Wong 1987)

and 0.05% (Burroughes 1990), are attributed to several factors including a

barrier to carrier injection at Al/PPV interface, high impurity levels, high

degrees of crystallinity, and the high work function of the electron injecting

electrode. The injection of electrons across Al/PPV interface has been a major

problem in fabricating stable PPV LED's with a long lifetime. Reaction of

aluminum atoms with the vinyl linkage of PPV (Fredricksson 1993 and

Dannetun 1993 and 1994) should facilitate charge transfer from aluminum into

the polymer. However, the existence of an interface layer between Al and PPV

results in a slower charge injection into the PPV film. The presence of this

interface, which is attributed to the reaction of PPV with oxygen (thus

preventing its reaction with Al), has been verified (Esteghamatian 1994-a and b) by utilizing impedance spectroscopy (Bottcher 1978 and Bruce 1987). By modifying the synthesis process this interface has been removed; thus facilitating charge transfer across the junction and enhancing device performance.

Crystallinity has been noted to reduce the light intensity in PPV LED's, (Yan 1994 and Son 1995). Son *et al.*, through incorporation of cis-linkage, introduced disorder into the PPV structure, and reported luminescence enhancement in PPV. In the current study, the increase in the cis-content of the polymer claimed by this group is argued, and more importantly, the nature and origin of crystallinity in PPV has been examined by utilizing transmission electron microscopy. The presence of some crystals embedded in an amorphous matrix was observed. However, it was noticed that the formation of PPV crystals originated from impurities which acted as nucleation sites. By careful examination of electron diffraction patterns obtained for these crystals, sodium chloride was found to be a major impurity. The presence of NaCl was also confirmed by using electron energy loss and x-ray spectroscopies. Therefore, in order to prevent crystallization, synthesizing a purer PPV

solution, however, seems to be less complicated than incorporation of cis-PPV

into the main chain, as was suggested by Son *et al.* The synthesis route

mentioned above has been slightly modified to exclude NaCl from the

precursor solution resulting in purer solutions, as will be discussed in chapters

2 and 4.

By evaluating and addressing some of the aforementioned problems,

efficiencies of up to 0.4 Lm/W have been attained. Moreover, device

instability has been studied and light emitting diodes based on PPV have been

fabricated which can operate under ambient conditions for more than 160

hours.

c) Photoconductivity and Carrier Generation Process

PPV is highly fluorescent and can be considered a good candidate for

photoconductors and xerographic applications. Despite numerous experiments

carried out by researchers, the mechanism of the photo-carrier generation

process in PPV is a subject of much debate (Bradley 1987-b, Rauscher 1990,

Lee 1993 and 1994, and Bassler 1995). In conventional photoconductors (e.g.

solar cells), which are p-n junctions mostly made of silicon (Si) , electrons are

excited into the conduction band creating unbound electron-hole pairs which can then move to the respective electrodes and, thus, create a current. In this theory, known as the band model, it is assumed that there is no coulombic attraction between the electrons and holes and, therefore, no electric field is required to dissociate e-h pairs. In the second model, known as the exciton model, photo-generated e-h pairs are bound and not free to move (dissociate) without the application of a strong bias voltage to the sample. By using delayed-collection-field and field-induced fluorescent quenching techniques, simultaneous measurements of fluorescent quenching and photoresponse have been made to provide more insight into the carrier generation process in PPV upon light excitation. Early results indicates that a strong electric field is required for e-h dissociation, supporting the formation of excitons upon light illumination. The detailed description of these techniques, the experimental procedures and results are presented in Chapter 3.IV.

1.2 Thesis Outline

This thesis includes six chapters. Chapter One, the introduction section, was presented above and the outline of the remaining chapters is as follows.

In Chapter Two the details of the experimental procedure; the synthesis process, the techniques and the equipment used for characterization and measurement are presented.

Chapter Three includes four parts each of which has been published or accepted for publication as a journal article. In Part I the conductivity of PPV, effect of doping, and the methodology for conductivity measurements have been discussed. In Part II, the colour changes in photoluminescence of PPV has been explored by varying the elimination time and temperature and by doping. Carrier transport in PPV and across a PPV/Al interface has been discussed in Part III. And finally, in Part IV two methods, fluorescent quenching and delayed-collection-field techniques, have been utilized to provide more insight into the nature of the excitation species in PPV upon illumination.

Chapter Four includes a comprehensive investigation of PPV morphology and crystallinity. By using transmission and IR spectroscopies, the degree of amorphousness and the origin of crystallinity in the polymer have been studied and the results have been compared to those of other

investigators.

In Chapter Five, light emitting devices have been fabricated, and instability, short lifetime, and low quantum efficiency of these devices have been investigated and addressed.

A summary of the thesis and the conclusions have been presented in Chapter Six. This chapter also includes recommendations for future work.
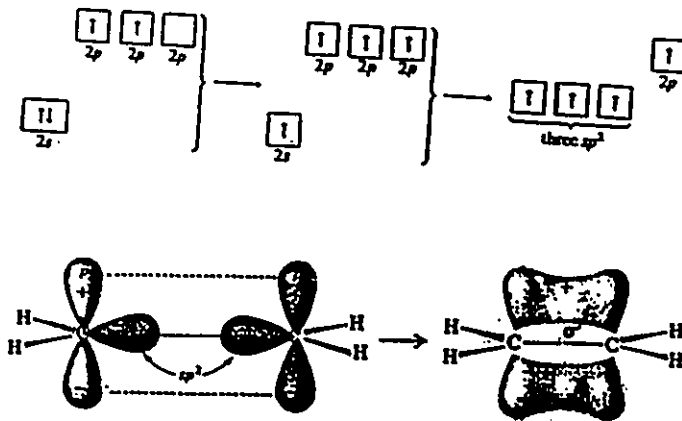
Fig. 1.1. Formation of sigma and pi bonds.
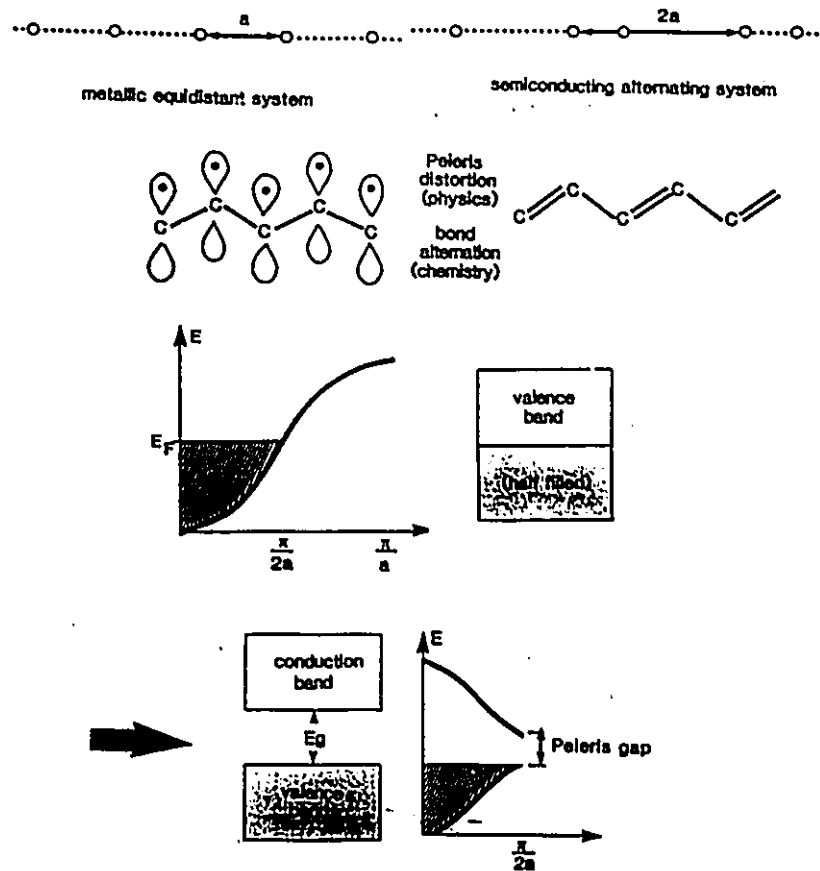
Fig. 1.2. Peierls' distortion theorem. Bond alternation results in lattice distortion which breaks the continuity of the energy bands and leads to formation of a band gap.

Chapter 2

Experimental Procedure

2.1 Synthesis of Poly(p-phenylene vinylene)

Synthesis of PPV via conventional methods results in an insoluble and infusible material which is not suitable for fabrication of thin film devices. An alternate method, the precursor route, has been utilized to prepare PPV films. In this method PPV precursor is first prepared and cast into the desired shape, and then, converted in a furnace. The conversion process is usually done at a high temperature and under a protective atmosphere, which will be mentioned later. Following is a detailed description of the synthetic process.

Synthesis of PPV via the solution processable precursor route is achieved in three major steps:

i) preparation of the sulphonium salt,

ii) polymerization, and

iii)elimination of unwanted sulphur products.

i) Preparation of Sulphonium Salt

Synthesis of the PPV building block was accomplished by mixing tetrahydrothiophene with α,α'-dichloro-p-xylene (3 to 1 mole ratio) in a water/methanol solution. The mixture was kept at 50 °C and stirred for 24 hours for the complete reaction to take place, see Fig. 2.1. The reaction product was concentrated by evaporation of excess water and methanol, and then quenched with cold acetone which immediately resulted in the precipitation of a white powder. After complete precipitation, excess acetone was removed and the precipitate was dried under vacuum at room temperature for a period of 1 to 3 days. The white hydroscopic powder, bis-sulphonium salt (MW=351.6 g/mole) thus obtained was weighed and a yield of about 79.9% was attained. The melting point of the compound was measured by the differential scanning calorimetry (DSC) technique and varied from 100 to 130 °C, as demonstrated in Fig. 2.2. The peak multiplicity in DSC measurements can have several causes among which recrystallization or the presence of two or more crystal sizes/structures can be mentioned (Bershtein 1994).

ii) Polymerization

The polymerization process to produce PPV was carried out by

preparing 0.5 M solution of the sulphonium salt in water/methanol solvent to which an equimolar equivolume amount of sodium hydroxide (initiator) was added. The solution was kept at 0°C and stirred for 1 hour under a vigorous flow of nitrogen to exclude oxygen. Immediately after adding the initiator, a highly viscous solution was formed which was diluted by addition of water/methanol mixture. Hydrochloric acid (0.5 N) was used to terminate the polymerization reaction. In order to remove monomer residues, sodium and chloride ions, and oligomeric compounds, the neutralized solution was dialysed against deionized water in dialysis tubes (Spectra/Por membranes) with molecular-weight-cut-offs (MWCO) of 12000 to 14000 Dalton. Use of dialysis tubes with MWCO less than these values (as suggested by Burroughes 1990 and Gmeiner 1993) resulted in a polymer with poor quality and presented serious problems in film casting and sample preparation. The dialysis time varied from 2 days to 4 weeks depending on the type of tube used. The clear viscous solution thus prepared is colourless and shows a blue colour under UV light. In some cases, due to oxidation and partial elimination, the colour of the solution changed to light green. The molecular weight of the polymer was estimated (from light scattering measurements) to be $\approx 10^5$ g/mole.

iii) Elimination

The elimination of thiophenium side group is an important step in the synthesis of a high quality PPV film. Time, temperature, and the atmosphere in which the elimination process is carried out are of major importance. In this step the as-cast and dried samples were placed in a home-made furnace operating under a protective atmosphere, vacuum or argon, at T>130 °C. The conversion temperature plays a more important role than the duration of elimination, since a complete conversion at low temperature requires a relatively longer time. The conversion time can be reduced by increasing the temperature at the expense of increased polymer oxidation and/or decreasing the intensity of the emitted light. The effect of time and temperature has been investigated and will be discussed in details in Chapters 3.II and 5.

2.2 Characterization; IR, UV-Visible Absorption & PL Spectroscopy

Infrared spectroscopy was carried out on free standing films of PPV by using a Bio-Rad FTS40 IR spectrometer. The free-standing films were prepared by casting the precursor solution onto Teflon substrates, which could then be peeled off. In general, preparation of free standing films was quite tedious. Glass slides treated with dichlorodimethylsilane $(CH_3)_2SiCl_2$, were

also used for film preparation. However, uniform and robust films could not

be obtained by this method. Due to the reaction of NaCl and PPV precursor,

sodium chloride could not be used as a substrate for preparation of PPV films.

Most of the IR spectroscopy was conducted on PPV films which were

prepared by casting the PPV precursor onto a highly polished AgCl substrate

(6 mm thick). The use of silver chloride, which is transparent from 4000 to

500 wavenumbers (2.5 to 20 μm), eliminates the need for free standing films.

The melting point of AgCl is 455 °C which is higher than the conversion

temperatures used here, and therefore, AgCl is an ideal substrate for IR

spectroscopy. The Perkin-Elmer LS-5 Fluorescent Spectrometer and UV-

Visible Absorption Spectrometer were employed to measure respectively

photoluminescence and absorption spectra of PPV films prepared on quartz

substrates (1 mm thick).

2.3 Crystal Structure Evaluation

The degree of crystallinity and quality of the PPV films were evaluated

using transmission electron microscopy (TEM). Samples for TEM were

prepared by spin-casting (at 1200 RPM) a dilute PPV precursor directly onto

copper grids which were evenly placed on a glass slide, see Fig. 2.3. The

copper grids were 3 mm in diameter having a mesh size of 200. The sample

was then heat treated at 300 °C for 12 hours in vacuum. While other methods

including microtomy were tried unsuccessfully, the aforementioned technique

for obtaining thin films required for TEM proved very effective. The film

thickness of the TEM samples were calculated using electron energy loss

spectroscopy (EELS) as $d \approx 33$ nm.

2.4 Doping Procedure

Doping of PPV was accomplished by using lithiumtriflate $LiCF_3SO_3$

and SO_3 as dopants. In the case of lithiumtriflate two doping methods were

employed. In the first method the electrolyte solution was spin-cast onto glass

slides under nitrogen and then converted at 255 °C in vacuum for 24 hours.

The samples were then immersed in 0.1 M $LiCF_3SO_3$ solution held at 65 °C for

various lengths of time. In the second method, solution-doped samples were

prepared by adding to the precursor a 0.2 M lithiumtriflate/methanol solution.

The solution was then cast and converted the same way as was mentioned

before. Doping with SO_3 was achieved by exposing free standing films of PPV

to the vapours of fuming sulphuric acid containing 30% free SO_3 for 24 hours.

2.5 Conductivity Measurements

Conductivity measurements were made on Al/PPV/Al cells by using an HP Impedance Analyser model 4248A, having a frequency range of 20 Hz to 1 MHz under an applied potential of 1.0 VAC. The temperature-dependence of the conductivity was determined by heating the samples in a custom-made furnace which was controlled by a Eurotherm temperature controller and interfaced with the impedance analyser via a personal computer.

2.6 I-V and EL Measurements

Light emitting devices were fabricated by casting or spin coating PPV solution onto ITO coated glass substrates (10-20 Ω/cm) supplied by Donnelly Inc., Holland, Michigan, USA. Prior to casting, the substrates were etched in a mixture of hydrochloric and nitric acids to obtain desired patterns. The PPV films were then converted in argon or in vacuum at various temperatures for several hours. Immediately after the elimination process, thin strips of Al (99.999%) or Mg (99%) about 2 to 6 mm wide, were thermally vacuum-evaporated onto the PPV films to form ITO/PPV/Al cells. Current-voltage (I-V) characteristics of these cells were measured by a Keithly Picoammeter model 485 and a Keithly Digital Multimeter model 177 DMM, both connected

to a DC power supply (Daystrom model IPW25), as schematically drawn in

Fig. 2.4. Light intensity was measured by a Minolta Luminance Meter LS-100.

The light spectrum and lifetime were measured using an optical fibre

connected to a monochromator and a photomultiplier tube which were

controlled by a personal computer.

For the sake of brevity, the details of photovoltaic experiments will not

be repeated here and the reader is referred to Chapter 3 Part IV.
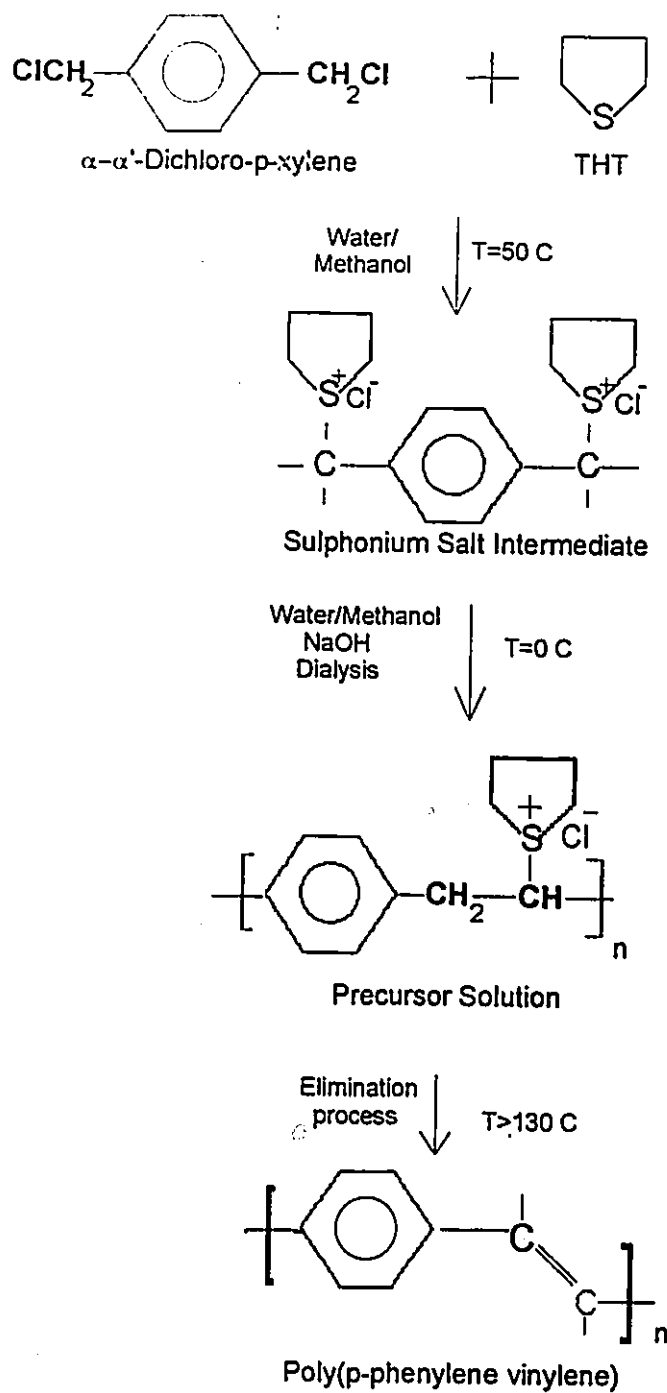
Fig. 2.1. Schematic Diagram showing PPV synthesis.
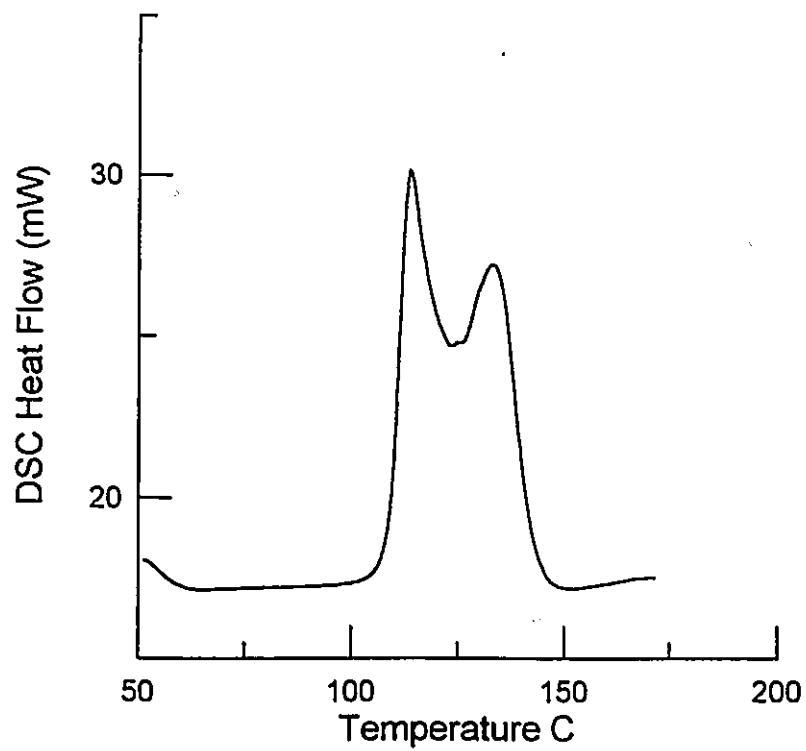
Fig. 2.2 DSC of PPV monomer
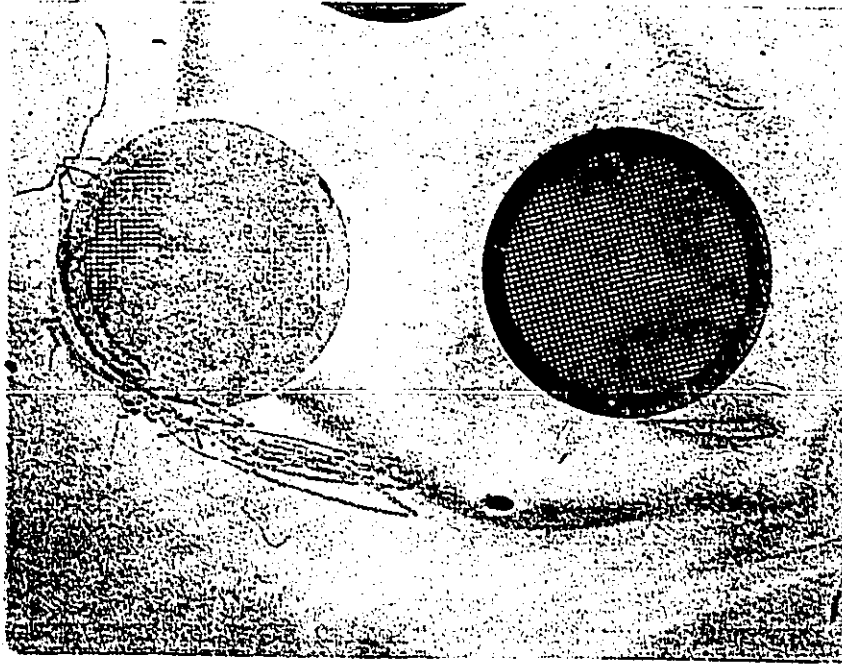
Fig. 2.3. A copper mesh and the trace of another one used for TEM (13X).
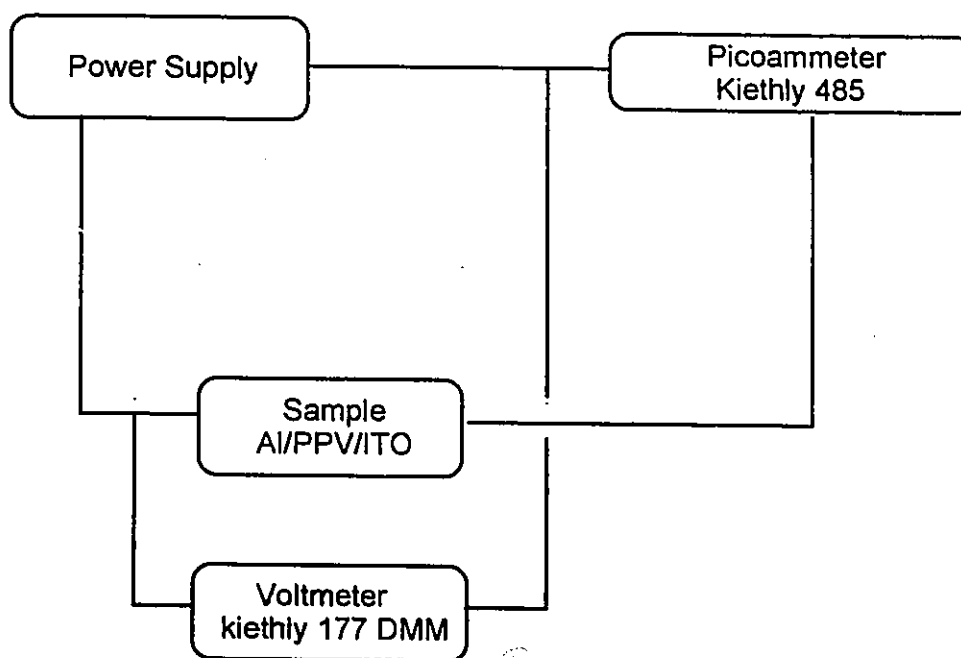
Fig. 2.4. Experimental set-up for current-voltage measurements.

Chapter 3

Published Results

Part I

Effect of Lithium Doping on the Conductivity of

Poly(p-phenylene vinylene)

McMASTER UNIVERSITY
Department of Materials Science and Engineering
1280 Main Street West, Hamilton, Ontario, Canada L8S 4L7
Telephone: (416) 525-9140 Ext. 4295/4293; Telex No. 0618347; FAX No. (416) 528-9295

Elsevier Sequoia
SA, PO Box 564
1001 Lausanne 1
Switzerland

November 17, 1995

Dear Publisher,

I am completing a Ph.D. thesis at McMaster University and I would like your permission to reprint the following articles in my thesis.

1) M. Esteghamatian & G. Xu, "Effect of lithium doping on the conductivity of poly(p-phenylene vinylene)", *Synthetic Metals*, 63 1994, pp195-197.

2) M. Esteghamatian & G. Xu, "Carrier transport in PPV and at a PPV/Al interface from impedance spectroscopy", accepted for publication June 27, 1995

I am also requesting that you grant an irrevocable, non-exclusive licence to McMaster University and to the National Library of Canada to reproduce these materials as part of the thesis. Proper acknowledgement of your copyright of the reprinted materials will be given in the thesis.

If these arrangements meet your approval, please sign where indicated below and return this letter to me. Thank you very much.

Sincerely

M. Esteghamatian

M. Esteghamatian

···

PERMISSION GRANTED FOR THE USE REQUESTED ABOVE

Authorized by: _____

Title: _____

Date: _____

Signature: _____

Permission is granted provided full reference is made to the original publication (journal title, volume, year, pages).

Signed: _____

Date: - 5 DEC. 1995

**ELSEVIER SCIENCE S.A.,
LAUSANNE, SWITZERLAND**

Chapter 3.I

Effect of Lithium Doping on the Conductivity of

Poly(*p*-phenylene vinylene)

M. Esteghamatian and Gu Xu

Materials Science & Engineering, McMaster University, Hamilton, Ontario,

Canada L8S 4L7

3.I.1 Abstract

The effect of lithium doping on the conductivity (σ) of Poly(*p*-phenylene-vinylene), PPV, has been studied via AC impedance measurements. PPV has been synthesized via a water soluble polymer electrolyte precursor. Its conductivity in both undoped and doped forms has been measured as a function of temperature. While doping with LiCl has not resulted in reliable data, doping with lithium triflate ($LiCF_3SO_3$) has improved the conductivity of PPV by more than two orders of magnitude. Plots of $\log(\sigma)$ versus $1/T$

show that the conductivities of undoped and doped PPV follow Arrhenius behaviour with equal activation energies, ($E_a \approx 0.37$ eV). The increase in conductivity without a change in the activation energy is attributed to the increase in the

electronic density of PPV.

3.I.2 Introduction

Poly(*p*-phenylene-vinylene), due to its high electrical conductivity and luminescence has been the subject of much research in recent years. Its high quantum yield, attractive mechanical properties and its ease of fabrication has made it a promising candidate for large area light emitting displays. The luminosity of PPV has been attributed to the π to π^* transition of the molecular orbitals of the double bonds and the electron-hole recombination that follows. This conjugated polymer has shown conductivities as high as 10^2 - 10^3 S/cm upon unidirectional stretching and doping with dopants such as I_2, SO_3, or AsF_5 (Murase 1984). These p-type dopants enhance electrical conductivity of PPV by increasing the number of charge carriers introduced into the π-electronic system through doping. Conduction in non-degenerate

ground state conjugated polymers (i.e. PPV) occurs via polarons and bipolarons. Upon doping, the number of radical ions and di-ions, which are chemical equivalents of polarons and bipolarons respectively, increases, thus enhancing the conductivity. Charge transfer is basically along the polymer chains. However, interchain conductivity also occurs via the hopping mechanism (Heeger 1988).

In the present report, the conductivity of Lithium-doped PPV has been studied using the AC impedance method, where not only the electronic but also ionic motion of the charge carriers can be probed. Due to its easy cation-anion dissociation, lithium triflate ($LiCF_3SO_3$) has been chosen to be the major dopant (Pak 1993-a and b).

3.I.3 Experimental Details

The synthesis of PPV via the polymer precursor route has been reported in detail elsewhere (Bradley 1987). The polymer electrolyte solution obtained by this method was cast onto ITO or aluminum-coated glass substrates, acting as electrodes, and dried under nitrogen to prevent oxidation of the polymer.

The film was then heat treated at 250°C for about 4 hours to remove unwanted sulphur products and increase the number of conjugated bonds. The light greenish film obtained after thermal treatment was then coated with aluminum under high vacuum. This coating served as the second electrode. Samples prepared by this method had satisfactory electrode-polymer contacts, which resulted in low contact resistance.

Doping was carried out prior to heat treatment by dissolving the proper amount of purified lithium trilate in deionized water and adding the solution to the PPV electrolyte.

Attempts were also made to use water-dissolved-LiCl as dopants. However, by forming little islands, LiCl precipitated out of the polymer and uniform films could not be obtained. The doped samples were heat treated similarly to the undoped ones. It was found that thermal treatment of doped samples at temperatures higher than 250°C resulted in burnt and punctured films. This, however, was not the case for the undoped PPV films. Infrared spectroscopy on free standing films of undoped PPV showed that the temperature and duration of heat treatment was enough to remove much of the

elimination (sulphur) products.

AC conductivity measurements were made by a HP impedance analyser (model 4248A) using a frequency scan of 20 Hz to 1 MHz under an applied potential of 1.0 volt. In order to avoid ionic motion across the interface, blocking electrodes were used. The samples were heated in a home-made furnace controlled by a Eurotherm temperature controller interfaced with the HP analyser via a multimeter and a personal computer.

3.I.4 Results and Discussion

The synthesis of PPV using the precursor route provides the flexibility of preparing samples in many forms - such as coatings, free standing films, foams and etc. By controlling the time and temperature of the heat treatment one can control the polymer structure (i.e. number of conjugated bonds), and thus, the final quality of the samples. It was found that conversion of undoped samples at temperatures higher than 250°C and holding times longer than 4 hours referred to by other investigators (Murase 1984) had little effect on the final results.

Characterization of the PPV films was done by infrared spectroscopy. The IR spectrum shown in Fig. 3.I.1 was carefully examined and the wavelengths at which these peaks occur were measured and compared with those of Bradley (1987). The absorption peaks including the trans-vinylene stretch and p-phenylene ring correspond with the ones reported by Bradley. However, there are some anomalies which should be addressed. The presence of the carbonyl group at 1688 cm^{-1}, which might be due to insufficient vacuum, indicates that the film was partially oxidized. Also, the peaks at 2940 and 2917 cm^{-1} show that the elimination was not entirely successful. However, the presence of a minute amount of the elimination products (as displayed by their relatively low intensities) even after long conversion times is unavoidable. The origin of the large absorption band between 3600 and 3000 cm^{-1} could be largely attributed to the unbound water molecules trapped in the polymer network (Li 1992). It should be emphasized, however, that despite these inconsistencies, the room-temperature conductivity of the PPV films measured here is in good agreement with the one previously reported (Murase 1984).

The AC impedance technique was employed to determine the contribution of all charge carriers to the conductivity of PPV. A typical Z'-Z" plot is depicted in Fig. 3.I.2, where Z' and Z" are respectively the real and imaginary part of the impedance. In general, each curve consists of two arcs. The first arc, in the form of a semi-circle, corresponds to the bulk conducting property of the polymer. The second one, in the form of a quarter of a circle to half a circle, represents the electrode-polymer interface impedance. Details of the analysis can be found elsewhere (Bruce 1987). The bulk DC conductivity is, therefore, simply determined by extrapolating the first arc to the Z' axis and reading the intercept.

The DC conductivities are plotted versus 1/T on a semi-logarithmic basis in Fig. 3.I.3. It is clear that doping with lithium has increased the conductivity of PPV by more than two orders of magnitude. Furthermore, logarithmic conductivities for both undoped and doped PPV vary linearly with reciprocal temperature, following the Arrhenius behaviour. The experimentally determined activation energies for undoped and doped PPV are essentially the same ($E_a \approx 0.37$ eV). In n-type doping charge transfer occurs from the donor (lithium) to the polymer chains, which act as a poly(anion). Judging from the

same E_a values, the increase in the conductivity is largely associated with the increase in the number of electronic carriers which are transported along the chains. Also, by bridging the gap between the chains, lithium ions can enhance the conductivity via hopping mechanism. The latter mechanism, however, seems to be less dominant.

3.I.5 Conclusion

Doping of PPV with lithium triflate has increased the d.c conductivity of PPV by more than 200 times. The experimentally determined activation energies for undoped and doped PPV were found to be the same, indicating that the enhanced conduction is largely due to the increase in electronic density rather than to the lithium ion motion within the polymer.
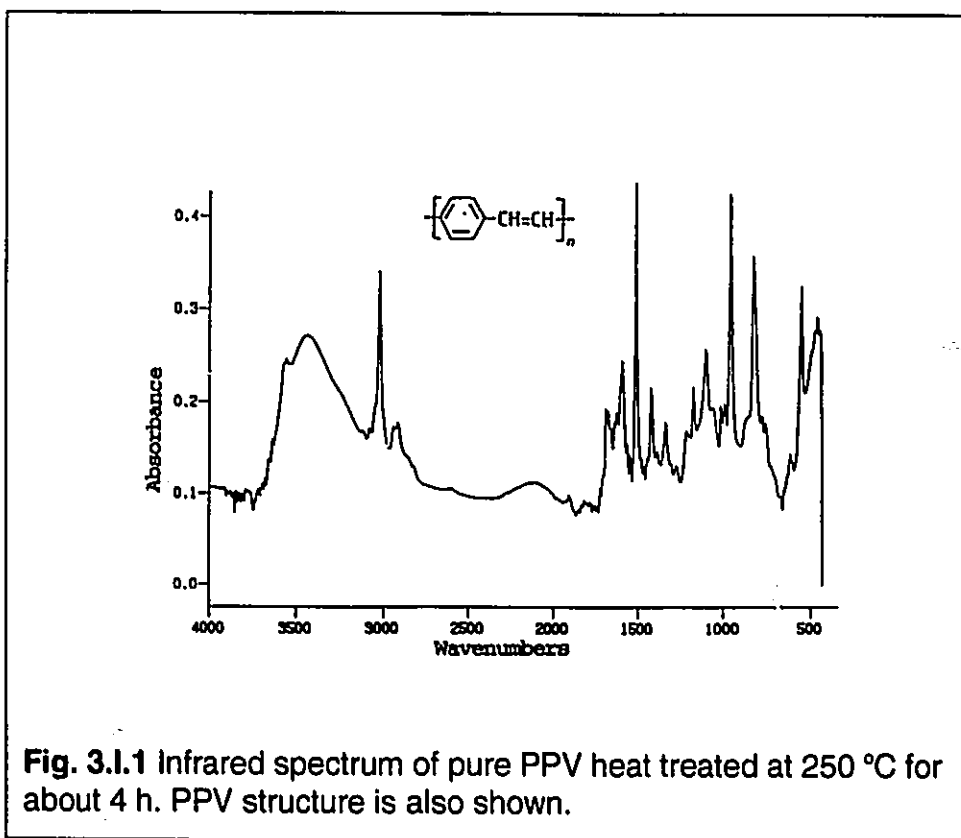
Fig. 3.I.1 Infrared spectrum of pure PPV heat treated at 250 °C for about 4 h. PPV structure is also shown.
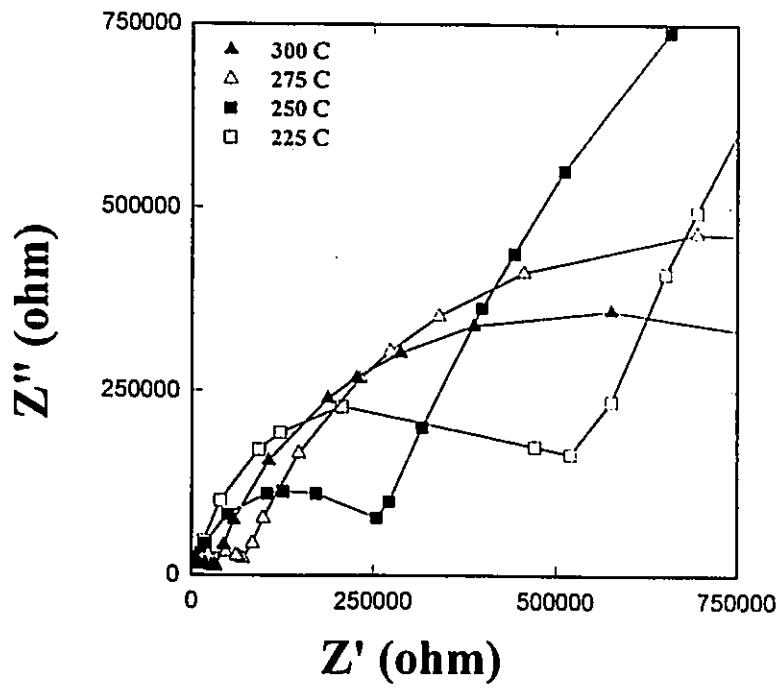
**Fig. 3.I.2 Typical plots of imaginary part of the impedance vs.
the real part. Each point on the graph corresponds
to one frequency.**
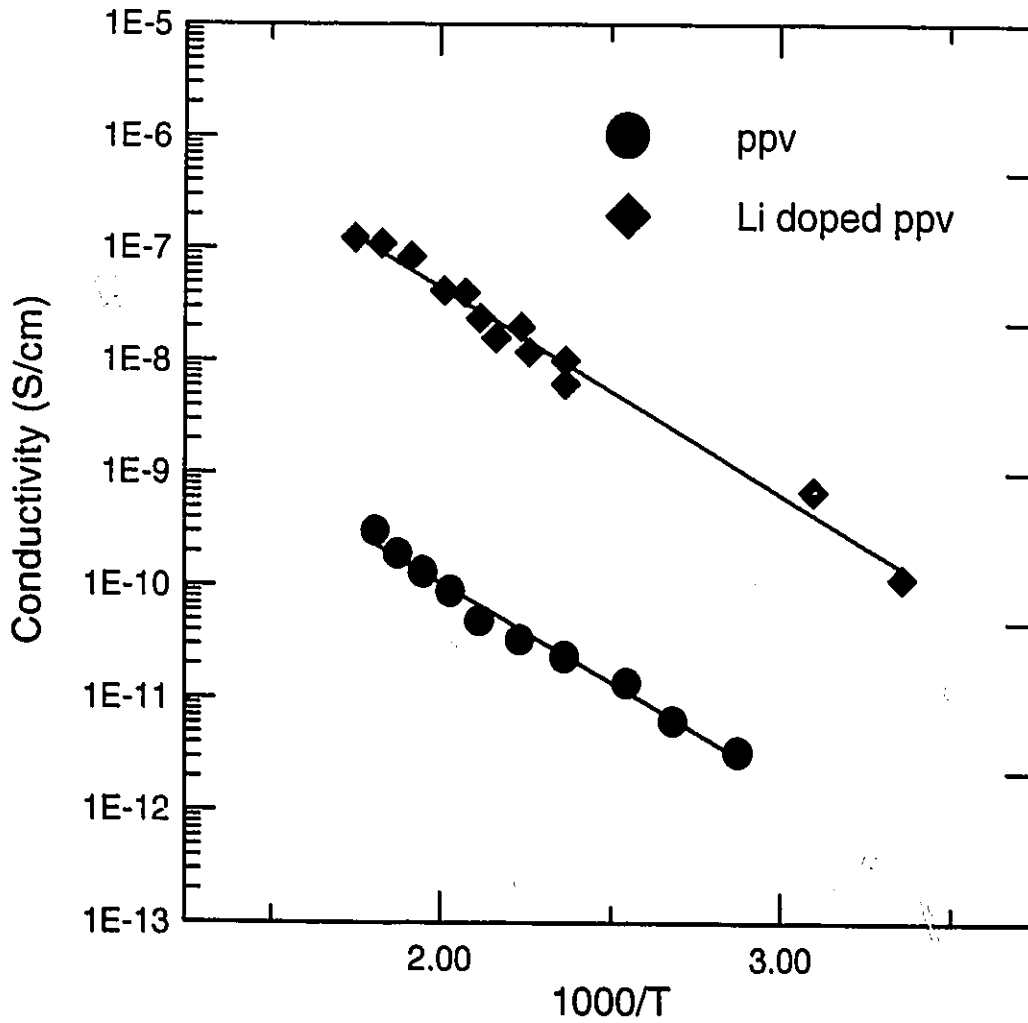
Fig. 3.I.3 Dc conductivity of PPV versus temperature.

Chapter 3

Published Results

Part II

Color Changes in Photoluminescence by

Doped, Unconverted and Partially Converted

Poly(p-phenylene vinylene)

This work was originally published in the

Appl. Phys. Lett. **65 (15), 10 October 1994, pp1877-1879.**

Where necessary modifications have been made to make

it consistent with the general theme of the thesis.

All the experimental sections;

synthesis, sample preparations, set-ups, and measurements

were entirely performed and contributed by the author

under direct supervision of Dr. Gu Xu. The

author also acknowledges some of the

initiatives contributed by Dr. Xu.

Copyright Permission
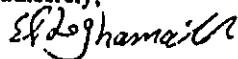
American Institute of Physics
Office of Rights and permissions
500 Sunniside Blvd.
NY 11797-2999

September 19,1995

Dear Publisher,

I request the permission for duplication of the following materials in my Ph.D. thesis.

M. Esteghamatian & G. Xu "Color changes in photoluminescence by doped, unconverted and partially converted poly(p-phenylene vinylene) ".

Applied Physics Letters 65 (15) 1877-1879 (1994).

Sincerely,

Esteghamatian

Mohammad Esteghamatian

Materials Science & Engineering
McMaster University
Hamilton, Ontario
Canada L8S 4L7

Phone 905-525-9140 (X27520)

Fax   905-528-9295

email   g9226411@mcmaster.ca
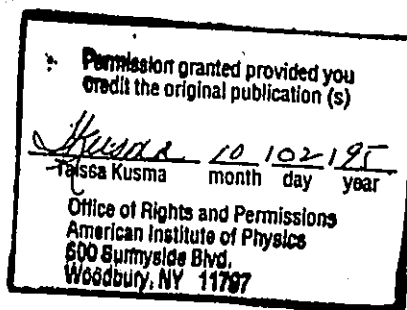
Chapter 3.II

Color Changes in Photoluminescence by

Doped, Unconverted and Partially Converted

Poly(p-phenylene vinylene)

M. Esteghamatian and G. Xu
Materials Science & Engineering, McMaster University, Hamilton, Ontario, Canada L8S 4L7

3.II.1 Abstract

Although green-light-emitting devices based on poly(p-phenylene vinylene) PPV, have been made and reported by several researchers, it is also of interest to design light emitting devices which emit light in various parts of the visible spectrum, particularly in the blue region. In this article the effect of doping and conversion time on the photoluminescence (PL) of PPV are investigated. It is observed that treating PPV films with sulphuric acid shifts the PL peaks to the blue region, and Li-doping red-shifts the spectra.

Unconverted and partially converted PPV films, on the other hand, show PL peaks at about 470 to 480 nm in the dark blue range. The shift in PL peak from green to blue is expected to be due to the decrease in conjugation length which determines the size of the band gap.

In search of blue-light-emitting devices, scientists have spent the last few years designing and modifying the architecture of some candidate polymers. PPV, the most promising candidate, has been intensely researched due to its processability, flexibility, and having a band gap in the green portion of the visible spectrum (Burroughes 1990, and Braun 1991). In display technology, however, a polymer (based on PPV) emitting blue light is of particular interest. A number of approaches including preparation of PPV derivatives such as poly(diphenylene diphenylvinylene) and synthesis of PPV block copolymers have been made by researchers (Bradley 1987, and Yang 1993) to modify the band gap of the electronic transitions, which control the color of the emitted light. In this investigation two methods for changing the color of the emitted light are studied. These techniques include doping and changing the conjugation length by varying the conversion times.

Thin films of PPV were spin coated on glass slides from a solution processable precursor prepared through polymerization of a sulphonium salt. The films were dried under nitrogen and heated up to 255 °C for 24 hours in a vacuum furnace. The samples were then immersed in 0.1 molar lithium triflate (LiCF$_3$SO$_3$) solution held at 65 °C. Solution doped samples were also prepared by mixing the precursor with a 0.2M lithium triflate-methanol solution so as to contain ≈0.014 w% lithium. It was noted that mixing the precursor with a more concentrated solution of lithium triflate resulted in a polymer precipitating out of the solution almost immediately. The conversion temperature was set at 255 °C since heat treatments at a higher temperature resulted in the degradation of the samples. Doping with SO$_3$ was carried out by exposing free standing films of converted PPV to fuming sulphuric acid containing 30% free SO$_3$ for 24 hours. Upon exposure, the samples immediately changed color from green to dark brown or black. Also, some deterioration of the samples were noticed. Unconverted films of PPV were prepared by casting, under nitrogen, the PPV solution onto glass substrate and storing them in vacuum prior to PL measurements. Partially converted films were also obtained by heat treating the as-cast samples at 300°C for 15

minutes, 2 and 24 hours. Heat treatment was performed in a vacuum furnace connected to a Eurotherm temperature controller with a ramp speed of 10 °C/min.

The PL measurements were performed at room temperature with a Perkin Elmer LS-5 Fluorescent spectrophotometer with the Xenon discharge lamp (8.3 W) as the source, pulsing at line frequency. The PL response of all samples prepared here were found insensitive to the excitation wavelength, and λ_{ex} was arbitrarily set at 355 nm. The excitation and emission slits for most of the experiments were set at 5 nm bandpass. The PL intensity of the unconverted films was found appreciably higher than the converted ones and, therefore, the emission slit for this case was reduced to 3 nm bandpass.

As shown in Fig. 3.II.1, diffusion doping of the converted films by immersing them in the lithium triflate solution has little effect on the PL spectrum of the films. The exposure times varied from one day to one week, and the general trend seems to be the broadening of the PL bands and gradual formation of single peaks emerging from the double peaks. The doping temperature was kept at 65 °C in order to prevent the evaporation of the doping

solution. However, higher doping levels are expected at elevated temperatures

and longer exposure times. Mixing of the PPV precursor with lithium triflate

prior to heat treatment, on the other hand, resulted in a more significant change

in the shape of the PL spectrum, as illustrated in Fig. 3.II.2. Disappearance of

the peak at 2.38 eV (504 nm) and a narrower band is observed from this

figure. Furthermore, the peak at 2.28 eV (526 nm) was red-shifted by 0.06 eV.

This may be attributed to the decrease in E_g as a result of the increase in the

number of n-type charge carriers, and the formation of the sub-gap polaronic

states. The decrease in the π-π^* transition gap size is also confirmed by the

four orders of magnitude increase in the conductivity of the solution-doped

PPV previously reported by the authors (Esteghamatian 1994-a) as shown in

Fig. 3.II.3.

Exposure of the PPV films to the fuming sulphuric acid blue-shifted the

first and the second peak by 0.07 and 0.13 eV respectively, as depicted in Fig.

3.II.4. The PL intensity of the emitted light was found much less than that of

the undoped samples, and the ordinates in Fig. 3.II.4 were readjusted for

comparison. Moreover, prolonged exposure of the PPV films to the fuming

sulphuric acid resulted in some deterioration of the films and loss of material

stability. Therefore, films obtained by this method can not be considered as good candidates for electroluminescence (EL) applications. The shift in PL peaks due to the exposure to fuming H_2SO_4 can be attributed to the reaction of SO_3 with conjugated bonds, and thus, reducing the number of double bonds, which consequently increases E_g.

Effect of conversion time on the PL spectrum of PPV was also studied. The PL data for unconverted and partially converted films are presented in Fig. 3.II.5. The as-cast samples showed a peak at 2.5 eV in the blue portion of the spectrum. Converting the films at 300 °C even for a few minutes shifted the spectrum to the yellow-green region. This shift may also be attributed to the increase in the number of conjugated bonds due to the elimination of the sulphonium group. It is noteworthy to mention that the PL intensity of as-cast (unconverted) samples was greater than the converted films by more than one order of magnitude.

Attempts were also made to measure the EL of the as-cast samples by placing the films between ITO and aluminum in a 1 MV/cm field. This experiment has been so far unsuccessful due to the ohmic resistance at the Al-

PPV interface, which causes the shorting of the EL cell and emission of blue sparks from the sample. Note that the PL spectra shown in Fig.3.II.5 have arbitrary units and the curves are offset for clarity.

Despite diffusion-doping, solution mixing was found to be an effective method of doping PPV with lithium triflate. The shift in the PL peaks of PPV due to Li-doping was attributed to the increase in the number of charge carriers and formation of the sub-gap polaronic states, which was also confirmed by the four orders of magnitude increase in conductivity. The blue shift in the PPV spectrum due to exposure to H_2SO_4 was obtained at the expense of the material properties and intensity, which makes them unsuitable for practical purposes. The unconverted films of undoped PPV showed high intensity peaks in the blue region of the visible range, and therefore, they can be considered as potential candidates for display applications. However, the effect of long term exposure to the air must be considered and studied before any useful device can be made.

Fig. 3.II.1. PL of PPV films immersed in 0.1M Li-triflate solution. Films were converted at 255 C for 24 h.

Fig. 3.II.2. Effect of Li doping on PL of PPV. Solution doping was performed with Li triflate prior to heat treatment. Films were converted at 255 C for 24 h.
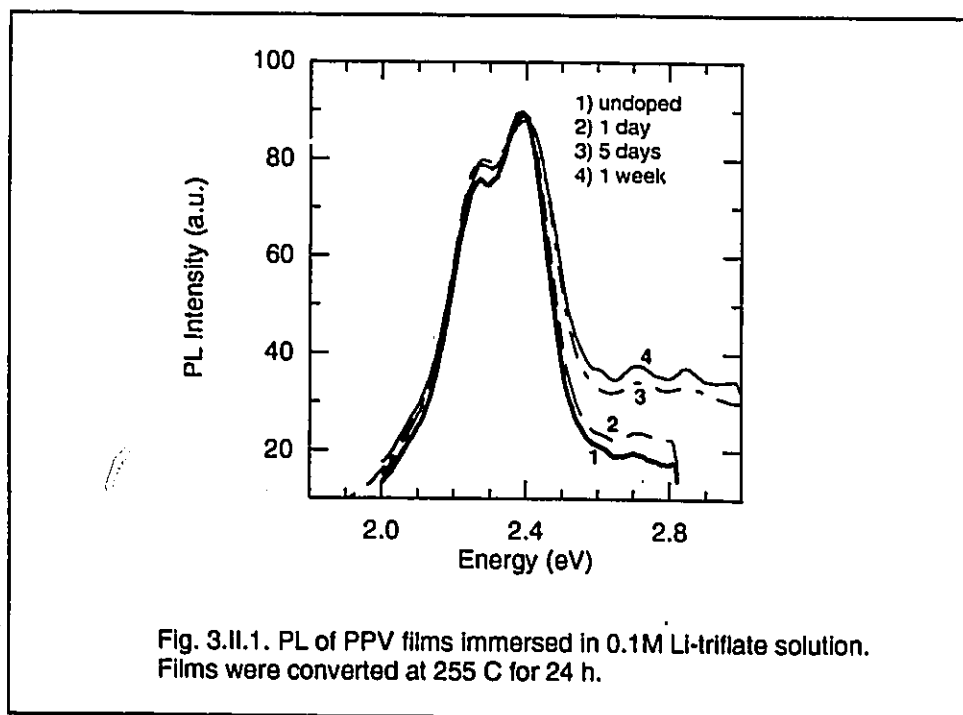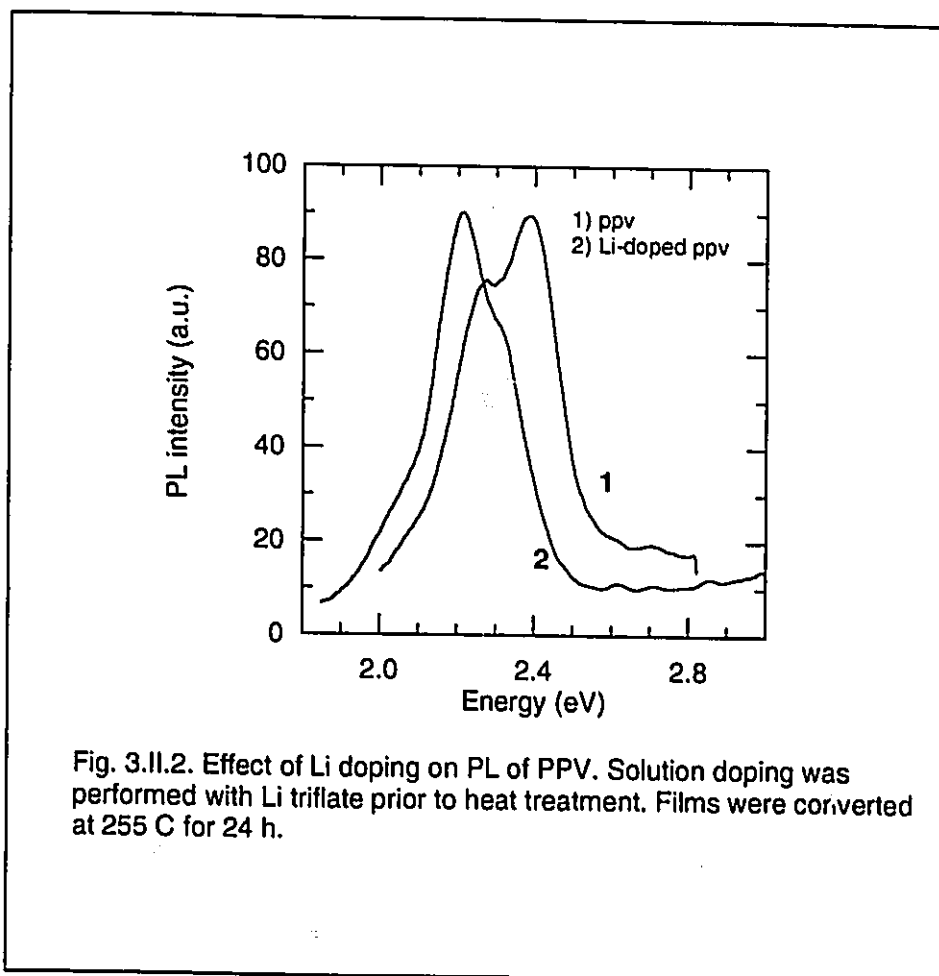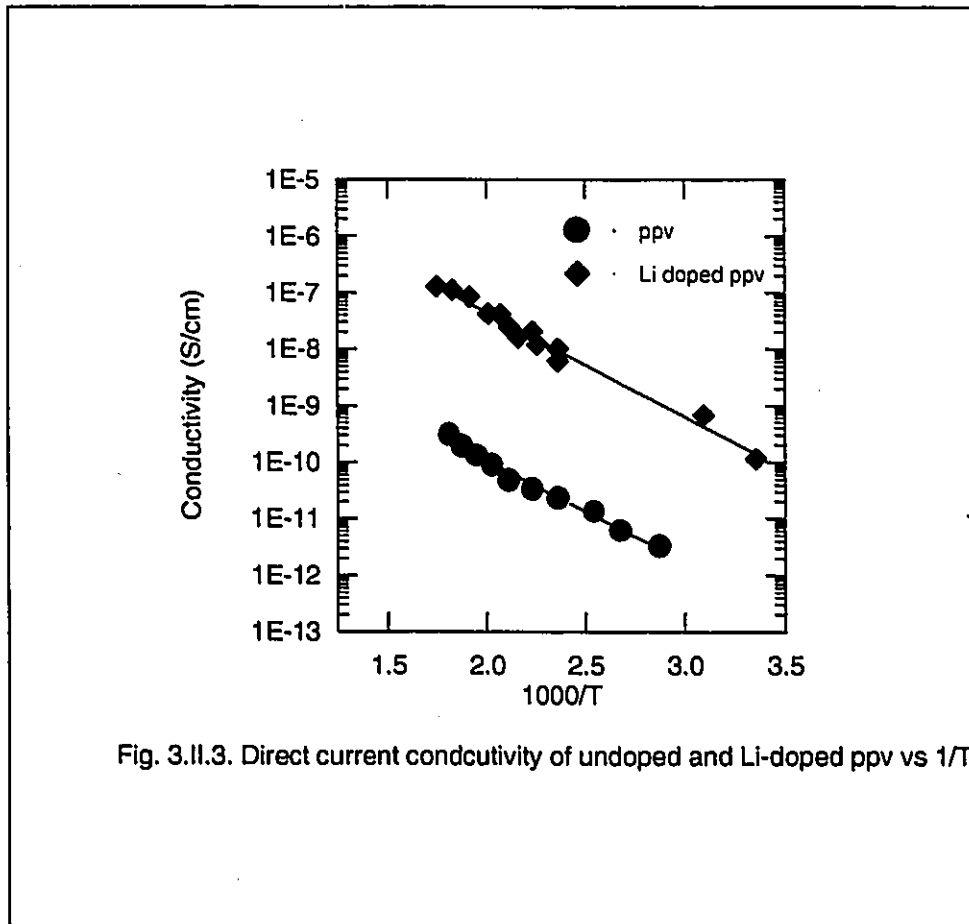
Fig. 3.II.3. Direct current condcutivity of undoped and Li-doped ppv vs 1/T.
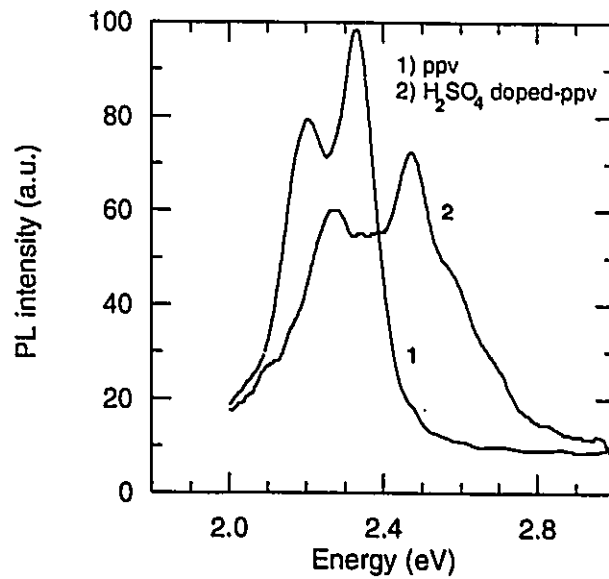
Fig. 3.II.4. PL spectrum of ppv treated with sulfuric acid. PPV films were converted at 300 C for 24 h and then exposed to sulfuric acid for 24 h.
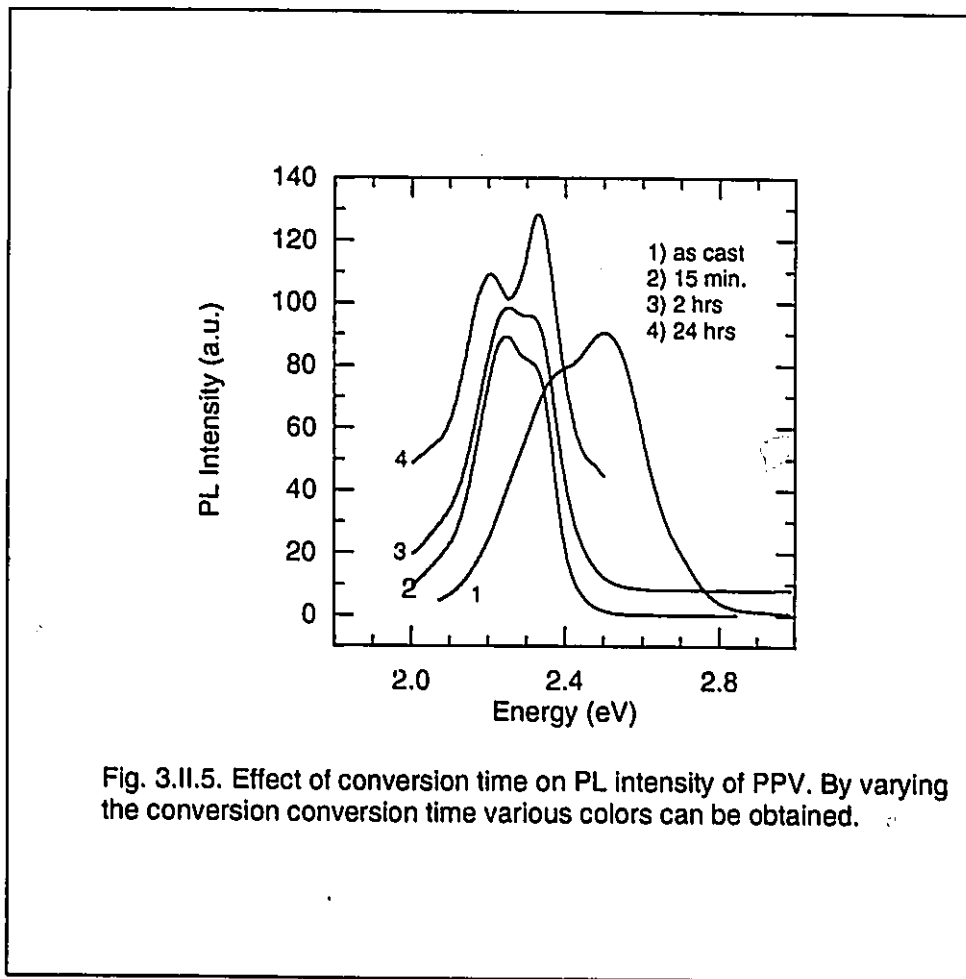
Fig. 3.II.5. Effect of conversion time on PL intensity of PPV. By varying the conversion conversion time various colors can be obtained.

Chapter 3

Published Results

Part III

Carrier Transport in PPV and at a

PPV/Al Interface From Impedance Spectroscopy

This work was originally published in

Synthetic Metals 75,1995, p 149-152.

Where necessary modifications have been made to make

it consistent with the general theme of the thesis.

All the experimental sections;

synthesis, sample preparations, set-ups, and measurements

were entirely performed and contributed by the author

under direct supervision of Dr. Gu Xu. The author also

acknowledges the contributions made by Dr. Xu in the

discussion and conclusion sections of this article.

McMASTER UNIVERSITY
Department of Materials Science and Engineering
1280 Main Street West, Hamilton, Ontario, Canada L8S 4L7
Telephone: (416) 525-9140 Ext. 4295/4293; Telex No. 0618347; FAX No. (416) 528-9295

Elsevier Sequoia
SA, PO Box 564
1001 Lausanne 1
Switzerland

November 17, 1995

Dear Publisher,

I am completing a Ph.D. thesis at McMaster University and I would like your permission to reprint the following articles in my thesis.

1) M. Esteghamatian & G. Xu, "Effect of lithium doping on the conductivity of poly(p-phenylene vinylene)", *Synthetic Metals*, 63 1994, pp195-197.

2) M. Esteghamatian & G. Xu, "Carrier transport in PPV and at a PPV/Al interface from impedance spectroscopy", accepted for publication June 27, 1995.

I am also requesting that you grant an irrevocable, non-exclusive licence to McMaster University and to the National Library of Canada to reproduce these materials as part of the thesis. Proper acknowledgement of your copyright of the reprinted materials will be given in the thesis.

If these arrangements meet your approval, please sign where indicated below and return this letter to me. Thank you very much.

Sincerely

M. Esteghamatian

···

PERMISSION GRANTED FOR THE USE REQUESTED ABOVE

Authorized by: _____

Title: _____

Date: _____

Signature: _____

Permission is granted provided full reference is made to the original publication (journal title, volume, year, pages).

Signed: _____

Date: - 5 DEC. 1995

**ELSEVIER SCIENCE S.A.,
LAUSANNE, SWITZERLAND**

Chapter 3.III

Carrier Transport in PPV and at a

PPV/Al Interface From Impedance Spectroscopy

M. Esteghamatian and G. Xu
*Materials Science & Engineering, McMaster University, Hamilton Ontario,
Canada L8S 4L7*

3.III.1 Abstract

Impedance spectroscopy has been used to study the charge transport

mechanism for poly(*p*-phenylene vinylene) and its interface with aluminum.

By separating the bulk and the interface contributions, the bulk and junction

resistance and capacitance have been determined at various temperatures. The

dependence of bulk DC conductivity on temperature yields an activation

energy of 0.36 eV, which implies that interchain hopping is the dominant

transport process in PPV. It is also found that the slower relaxation process

occurs at the interface, which limits the carrier injection across Al/PPV

junction. The observation of high interfacial resistance and low electron

mobility in PPV leads to the conclusion that most of the e-h recombination occur at the Al/PPV junction, thus lowering the efficiency and life time of electroluminescent display devices based on PPV.

3.III.2 Introduction

In recent years, the attractive opto-electronic properties of some conjugated polymers has generated interest in their use in large area displays. Poly(p-phenylene vinylene) PPV, due to its ease of fabrication and light emission in the yellow-green portion of the visible spectrum, has been intensely studied. This polymer, however, suffers from short lifetime and low efficiency. Researchers have tried to address and overcome some of these problems. For example, by using calcium or magnesium instead of aluminum contacts as the electron injecting electrode, the electroluminescent (EL) efficiency can be considerably improved (Marks 1993). Electrodes such as Ca are, however, highly reactive with oxygen and pose serious problems in manufacturing such devices. Aluminum, on the other hand, is easier to work with, has been widely used in the semiconductor industry, and can be considered a good candidate - provided that the low efficiencies associated

with Al and the highly capacitive nature of Al/PPV interfaces are addressed.

In the present work, impedance spectroscopy is employed to study the

transport processes in PPV and across Al/PPV junctions. In this method

complex resistivity (impedance), arising due to the phase lag between the

current and the applied AC voltage, is measured at various frequencies. By

plotting the imaginary part (Z") against the real part (Z') of the impedance,

non-trivial information pertinent to the system can be obtained (Bruce 1987).

Moreover, the AC impedance technique allows us to isolate the bulk and the

interface properties and analyze them individually.

In conventional PPV based LED's the polymer is usually sandwiched

between ITO and aluminum electrodes. However, in order to understand the

Al/PPV interface, in the current study PPV films were placed between two

aluminum electrodes, thus eliminating the contribution to the interface

capacitance from the ITO/PPV junction. Furthermore, since some aluminum

oxide is usually formed during Al-electrode deposition, it is desirable to

investigate its role on the Al/PPV interface and on device performance.

Therefore, aluminum-coated glass substrates prepared under vacuum were

exposed to air and a thin layer of aluminum oxide was intentionally formed on

top of the Al layer, and the impedance of the final cell ($Al/Al_2O_3/PPV/Al_2O_3/Al$) was measured as a whole. It should be mentioned that the aluminum oxide layer on the bottom electrode is thicker than the oxide layer on the top electrode, however, the series capacitances of the two electrodes can be represented by a single capacitance.

3.III.3 Experimental Detail

PPV solution was prepared according to the standard precursor route through polymerization of a sulphonium salt. The solution was then cast onto Al-coated glass substrates and dried under nitrogen to prevent oxidation of the polymer. The samples were then converted at 250°C for 4 hours in a custom-made vacuum furnace controlled by a temperature controller having a ramp speed of 10°C/min. Infrared and UV-visible spectroscopy of free standing films prepared under the same conditions showed that the temperature and duration of heat treatment was sufficient to remove much of the elimination (sulphur) products. Top electrodes were made by evaporating aluminum (99.999%) onto the PPV films (Esteghamatian 1994-a).

Impedance measurements were made by a HP impedance analyzer (model 4248A) using a frequency range of 20 Hz to 1 MHZ under an applied potential of 1.0 volt AC. The samples were heated in a furnace interfaced with the HP analyzer via a multimeter and a personal computer.

3.III.4 Results and Discussion

The impedance plots of PPV at temperatures ranging from 100 to 300°C are shown in Fig. 3.III.1. As is seen the cole-cole plots at high temperatures (i.e. 275°C) take the form of two semicircles, which may be represented by a parallel combination of the bulk resistance (R_b) and capacitance (C_b) in series with a parallel arrangement of the junction resistance (R_j) and capacitance (C_j), as shown in Fig. 3.III.2.a. The impedance data at low temperature consists of a semicircle and a spike. The circuit equivalent of this case can be approximated by a parallel arrangement of R_b and C_b in series with C_j (Fig. 3.III.2.b). The spike mentioned above should under ideal conditions be vertical. However, deviations from ideality occurs due to (for example) rough metal-polymer interface (Bruce 1987). Although, through curve fitting many combinations of RC circuits can be found to match the data, the circuit

equivalent employed here is the simplest and most widely used for solid electrolytes sandwiched between two similar blocking electrodes. Furthermore, due to the highly capacitive nature of the interface, especially at low temperature, the semicircles associated with the junction are considerably larger than, and overlap with, the semicircles related to the bulk, and the process of extracting accurate information from the low temperature data becomes questionable. Therefore, in this study the RC circuit shown in Fig. 3.III.2.a has been utilized to obtain information at high temperature and extrapolate to low temperature where necessary.

The junction capacitance mentioned above is thought to arise mainly due to the presence of Al_2O_3. This is because the junction capacitance obtained experimentally as $C_j=10^5$ pF corresponds well to the value obtained from the following equation,

$$C_j=\epsilon\epsilon_o A/d$$

in which ϵ is the dielectric constant of Al_2O_3, ϵ_o is the vacuum permittivity, A is the contact area and d is the thickness of the aluminum oxide (estimated to be about 2 to 5 nm). Taking $\epsilon=10$, $\epsilon_o=8.85$ pF/m, $A=5$ mm^2, the junction

capacitance is calculated as $C_j=8.85*10^4$ pF, which is very close to the experimentally determined interface capacitance.

The bulk DC conductivity ($\sigma_{DC} \propto 1/R_b$) thus obtained is plotted versus reciprocal temperature in Fig. 3.III.3. The activation energy calculated by using Arrhenius model is ≈ 0.36 eV, which is much less than the energy gap ($E_g \approx 2.4$ eV). Therefore, conduction models other than the band theory should be considered. Also, since PPV, unlike polyacetylene, is non-degenerate, charged solitons (polarons) in the polymer are confined and their motion giving rise to long range conduction may be ruled out. The low activation energy points out the possibility of carrier transport through hopping between localized states in a disordered fashion, i.e. via interchain rather than intrachain conduction. These localized states can be polarons, clusters of impurity ions, structural defects in the polymer and etc.

Assuming that hopping is the dominant process, the DC conductivity of PPV should be less than the AC conductivity. This is demonstrated in Fig. 3.III.4, where the bulk AC conductivity $\sigma_{AC}(\nu,T)$ is plotted against frequency (ν) at various temperatures. The bulk AC conductivity was determined by

using the values from the first semi circles drawn in Fig. 3.III.1 and taking into account the contact area and thickness. As is seen, at low frequencies the conductivity is more or less independent of v and after a sharp increase seems to reach a plateau. An unusual feature of this graph is that at high frequencies the AC conductivity decreases with increasing the temperature. The origin of this decrease is not known, however, it is speculated that with increasing temperature and frequency, thermally-activated and frequency-activated hopping processes do not constructively contribute to the charge transport, and may in fact increase the mean free path for the charge carriers and decrease the hopping probability. This statement can, to some extent, be substantiated due to the fact that more than one relaxation process is present in disordered systems. A careful examination of the impedance plots depicted in Fig. 3.III.1 demonstrates that the centre of an imaginary circle fitted through the bulk impedance is depressed below the x-axis, indicating that more than one relaxation time (τ) is present in PPV (Anderson 1964). In short, several hopping mechanisms, inter-soliton hopping or hopping between unspecified localized states may give rise to conduction, and with increasing T and v, some of these processes may interfere with one another.

The process of extracting the AC conductivity is rather complicated and is beyond the scope of this paper. However, it is noteworthy to mention that the AC conductivity can not be simply determined by subtracting the DC conductivity from the total conductivity, i.e.,

$$\sigma_{AC}(v,T) \neq \sigma_t(v,T) - \sigma_{DC}(v,T)$$

This is because the subtraction is based on the assumption that hopping processes responsible for long range DC conductivity have a single relaxation time and do not contribute to the v-dependent conductivity, which (as was mentioned) is unrealistic in disordered systems (Ngai 1986).

The mean relaxation times (τ_a) for the bulk and the interface are plotted against $1/T$ on a semi-log scale in Fig. 3.III.5. Assuming that τ_a exponentially varies with $1/T$, the activation energies for the bulk and the junction relaxations are determined as 0.20 and 0.33 eV, respectively. The higher activation energy and the longer relaxation times associated with the junction indicate that charge transport across the interface is the limiting factor in

controlling the conduction process. Furthermore, the highly capacitive Al/PPV interface, evident in Fig. 3.III.1, leads to positive and negative charges to build up at the interface. Consequently, in an EL device based on PPV (e.g. AL/PPV/ITO), the majority of the electron-hole recombination (radiative and non-radiative) takes place at the interface between Al and PPV. The non-radiative processes, however, produce heat which in turn results in degradation of the polymer or the contact, thus shortening the lifetime of the device. In addition, photons generated from the radiative recombination at the junction have to travel first through the polymer and then through the transparent electrode (ITO) to reach the detector. In the process they lose much of their intensity as a result of the internal reflections and absorptions, hence lowering the efficiency.

3.III.5 Conclusions

Hopping between localized states is thought to be the major carrier transport mechanism in PPV. These localized states, which have energies within the band gap, lower the efficiency by acting as quenching sites (traps). Highly pure and conjugated PPV with least structural defects is thus required

to achieve significant efficiencies. The highly capacitive Al/PPV junction provides interfacial electron-hole recombination, which lowers the lifetime and efficiency of electroluminescent displays. It is believed that the quality of the interface is detrimental to fabrication of commercially viable devices, and more investigation to improve the interface is in order.
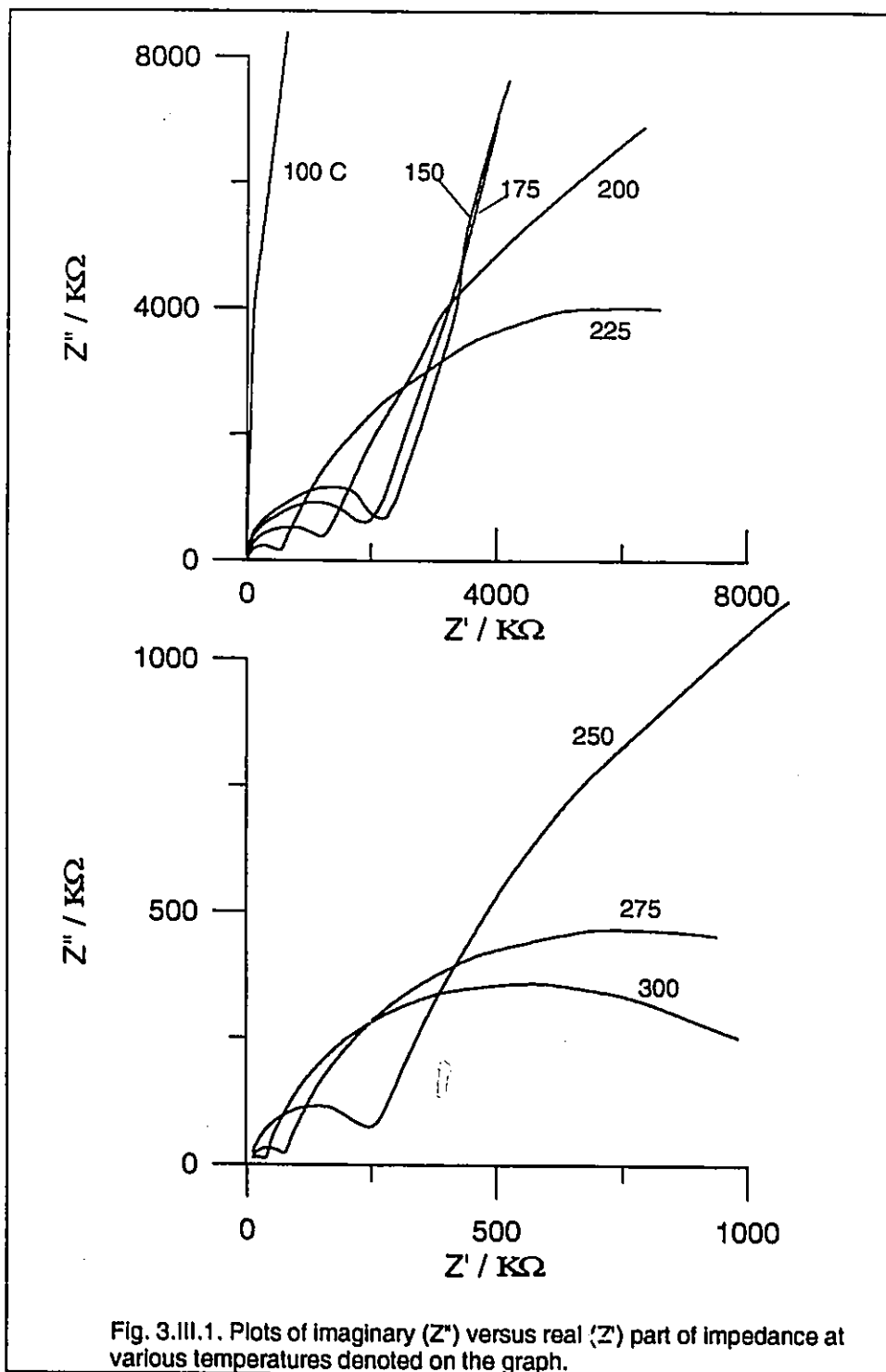
Fig. 3.III.1. Plots of imaginary (Z") versus real (Z') part of impedance at various temperatures denoted on the graph.
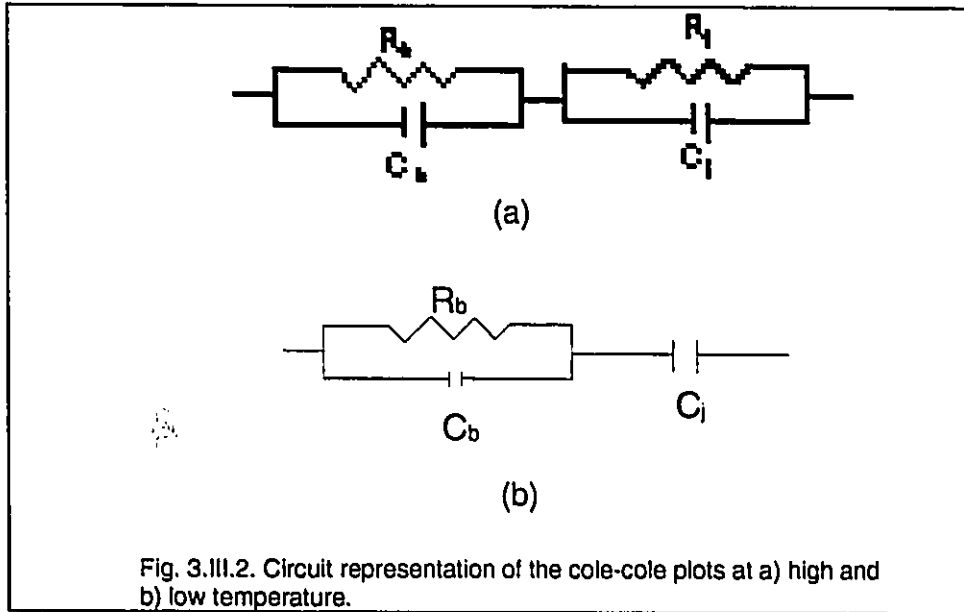
Fig. 3.III.2. Circuit representation of the cole-cole plots at a) high and b) low temperature.
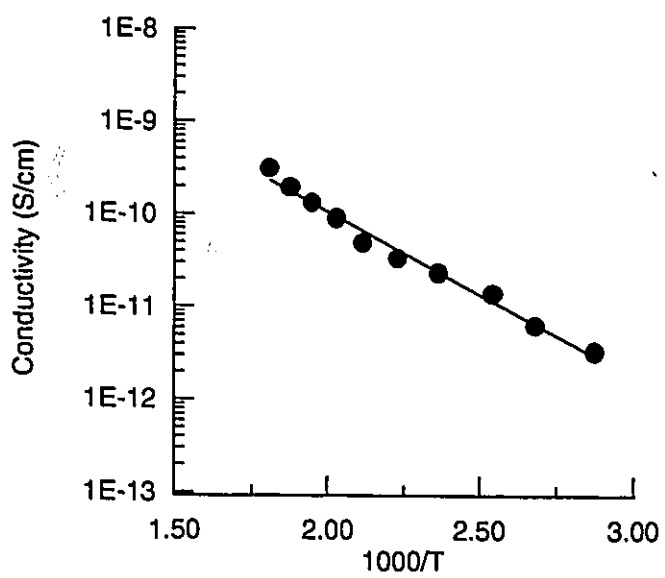
Fig. 3.III.3. DC conductivity of PPV versus inverse temperature.

Fig. 3.III.4. Frequency and temperature dependence of the bulk conductivity.
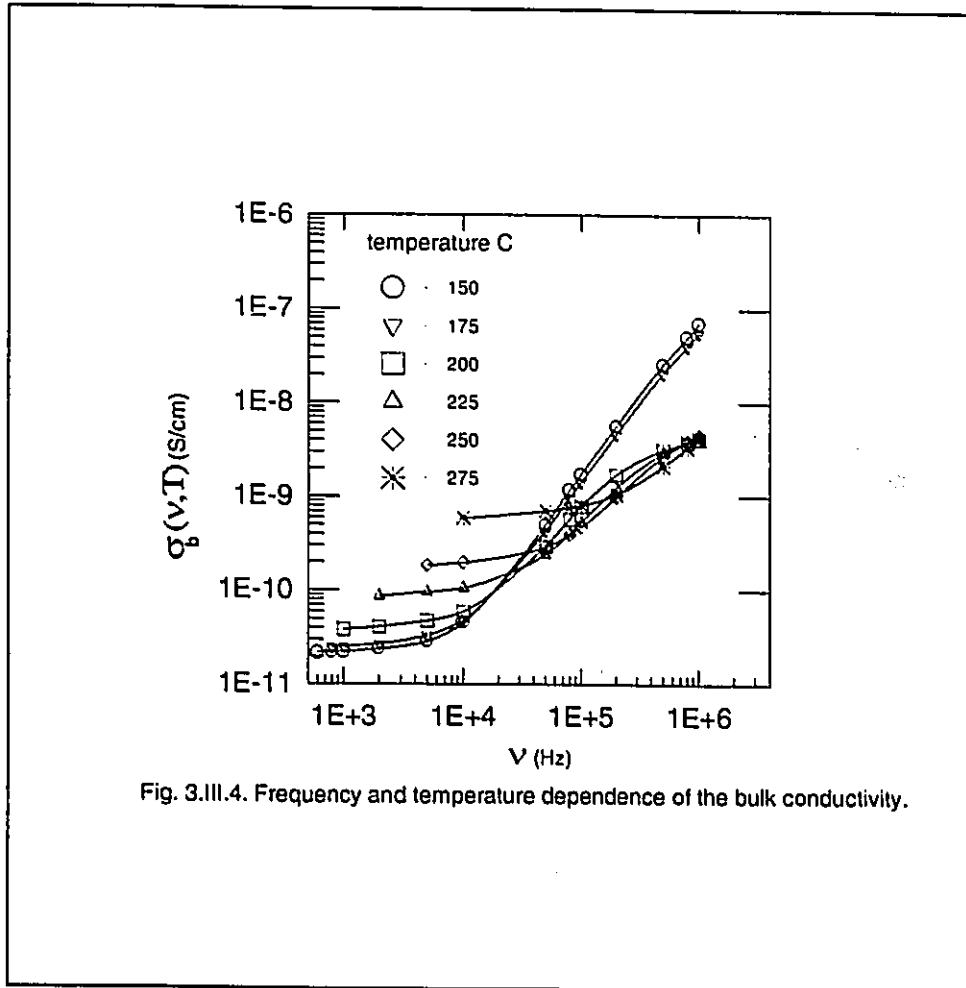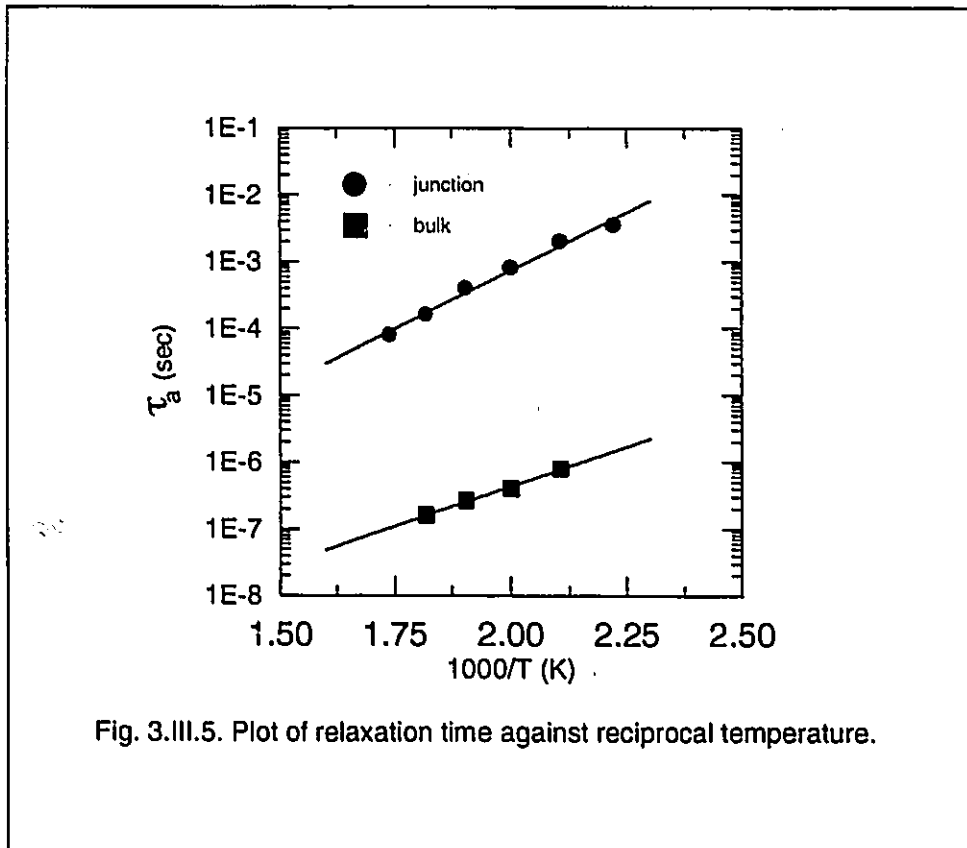
Fig. 3.III.5. Plot of relaxation time against reciprocal temperature.

Chapter 3

Accepted Results

Part IV

Study of Carrier Generation Process in

Poly(*p*-phenylene vinylene) by Fluorescent Quenching

and Delayed-Collection-Field Techniques

This work has been accepted for publication by the

Journal of Physical Chemistry in March 1996.

Where necessary modifications have been made to make

it consistent with the general theme of the thesis.

All the experimental sections;

synthesis, sample preparations, and measurements

were entirely performed and contributed by the author

under direct supervision of Dr. Gu Xu and Dr. Zoran Popovic of Xerox

Research Center of Canada. The author also acknowledges Dr. Popovic's

contributions in the experimental set-up

and measurement sections.

Chapter 3.IV

Study of Carrier Generation Process in

Poly(p-phenylene vinylene) by Fluorescent Quenching

and Delayed-Collection-Field Techniques

M. Esteghamatian[*], Z.D. Popovic[+] & G. Xu[*]

Materials Science & Engineering Dept., McMaster Univ., Hamilton, Ontario, Canada L8S 4L7

+Xerox Research Centre of Canada, 2660 Speakman Drive, Mississauga, Ontario, Canada L5K 2L1

3.IV.1 Abstract

Carrier generation process in poly(p-phenylene vinylene) PPV, has been investigated by using field-induced fluorescent quenching and delayed-collection-field techniques under pulsed illumination. Relative photoresponse and fluorescent quenching have been measured at electric fields of up to 300 V/μm. The results demonstrate a linear relation between fluorescent quenching and photoresponse at high electric fields, indicating that almost all field-quenched excited states lead to carrier generation. Experimental results also indicate that most of photogenerated electron-hole (e-h) pairs have a lifetime

of less than several μs and majority (70%) of them decay non-exponentially to ground state in about 1 ms after illumination. Fluorescent quenching and carrier generation efficiencies obtained at the highest applied electric field are 34% and 42% respectively. Results also suggest that carrier generation in PPV is a two step process. In the first step excited singlet states dissociate into bound geminate e-h pairs, and in the second step the geminate pairs are separated into free carriers. Both steps are influenced by applied electric field.

3.IV.2 Introduction

The attractive optoelectronic properties of PPV make it a good candidate for a variety of technological applications. Moreover, the synthesis of this conjugated polymer via the water-soluble precursor route provides the flexibility to easily fabricate electronic devices. Light emitting diodes based on undoped or doped PPV can now emit light in various parts of the visible spectrum. Other potential applications of PPV are in photoconductors and xerographic devices. Although photoconductivity and mechanism of carrier generation in PPV has been intensely researched in recent years, the exact nature of the process, free carrier generation versus exciton model, is yet to be

resolved. Eckhardt showed that in several conjugated polymers including PPV the threshold of photoconductivity (PC) coincided with the onset of photoabsorption (PA). Lee, by conducting steady state and picosecond photoconductivity experiments verified this agreement and concluded that photoexcitation in PPV led to direct generation of free carriers through interband π-π* transition; a process analogous to interband excitation in inorganic semiconductors. The agreement between PC and PA thresholds, however, can not be simply taken as the evidence for photogeneration of free carriers (Bassler 1995). This coincidence can be merely due to the extrinsic rather than intrinsic charge carriers. Using delayed-collection-field technique, this study has been conducted to provide more insight into the field-induced fluorescent quenching and carrier generation process. In order to directly evaluate the correlation between fluorescent quenching and photoresponse, simultaneous measurements of the two quantities have been made.

3.IV.3 Experimental Detail

PPV solution was synthesized by mixing α,α'-dichloro-p-xylene and tetrahydrothiophene according to the standard precursor route. A slight

modification was, however, introduced by using dialysis tubes with molecular-weight-cutoffs of 12000 to 14000 Dalton. The solution was then cast onto substrates and converted in vacuum at 260°C for 24 hours. Fig. 3.IV.1.a represents the cell configuration in which PPV is sandwiched between two insulating layers. These layers, SiO_x and Goodyear OMS pliolite (dissolved in cyclohexane), were used to block the carrier injection from the electrodes into the sample, thus enabling us to study the carrier generation process in the PPV film only.

In the delayed-collection field measurements of the photoresponse, a bias voltage (V_{appl}) is applied to the sample and the sample illuminated by a pulsed light source. Immediately after light excitation (i.e. after a 0.1µs or 0.1ms delay in the current experiments), a constant collection voltage (V_{coll}) is applied and the voltage drop at the electrodes is measured. Furthermore, fluorescent signals are simultaneously detected. Finally, by varying the bias voltage, photoresponse and fluorescent quenching are measured as a function of the applied field. All equipment required for this experiment including power supplies, pulsed light sources, a monochromator and etc. are controlled

by a personal computer. The waveform of the applied electric field together

with the timing of the pulsed light is illustrated in Fig. 3.IV.1b. For the

description of the circuit diagram used in the aforementioned technique see the

appendix of the work by Popovic (1983). The sample was illuminated from the

NESA side by either a white light from a pulsed xenon lamp or by the third

harmonic of a Nd/YAG laser (λ=355nm). In both cases the results were

consistent. As was mentioned before, in measuring fluorescent quenching and

photoresponse, the collection delay time, time delay between pulsed excitation

and charge collection, was set to $0.1\mu s$ for laser excitation and to $0.1ms$ for

white light illumination. In the time evolution experiments, the delay time was

varied over several decades ranging from $0.1\mu s$ to 10ms and pulsed laser

excitation was used.

The UV-visible absorption and photoluminescent spectra of each

component were separately measured to ensure that light absorption and

fluorescent emission from the insulating layers and NESA (tin oxide) were

negligible compared to those of PPV, as illustrated in Fig. 3.IV.2. The sample

thickness d, was calculated by using capacitance method ($C_p = \epsilon_o \epsilon A/d$) to be

approximately 2 microns. The dielectric constant of PPV was taken from

literature (Antoniadis 1994) as $\epsilon=3$, and the sample area and capacitance were measured as $A=40.323$ mm^2 and $C_p=495$pF respectively. All measurements were performed in the dark at room temperature under a gentle flow of nitrogen over the cell surface. The use of nitrogen significantly increases the cell break-down voltage. Quantities measured were the relative photoresponse (voltage drop normalized to the incident light intensity),

$$PR=\Delta V/I_{light} \tag{3.IV.1}$$

and fluorescent quenching, defined as,

$$\phi(E) = \frac{I_f(0) - I_f(E)}{I_f(0)} \tag{3.IV.2}$$

where $I_f(E)$ is the fluorescent signal normalized to the incident light intensity at the electric field E applied to the sample. It should be mentioned that the relative photoresponse PR, and carrier generation efficiency η, are related through a constant as,

$$\eta(E)=C * PR(E) \tag{3.IV.3}$$

A simple kinetic model (Popovic 1983 and 1985) gives the correlation

between $\phi(E)$ and $\eta(E)$ as,

$$\phi(E) = \frac{\eta_G(E) - \eta_G(0)}{1 - \eta_G(0)} \qquad\qquad (3.IV.4)$$

where $\eta_G(E)$ is the quantum yield for the geminate e-h pairs. The quantum

yield of the free carriers is given by,

$$\eta(E) = \Omega(E)\,\eta_G(E) \qquad\qquad (3.IV.5)$$

where $\Omega(E)$ is the dissociation probability of geminate e-h pairs. At high fields

$\Omega(E)=1$ and $\eta(E)=\eta_G(E)$, and thus linear relationship between $\phi(E)$ and

$\eta(E)=C*PR(E)$ is expected. By using this linear correlation (Eq. 3.IV.4) at

high fields, the constant C can be determined and relative photoresponse data

can be scaled to attain true carrier generation quantum efficiency.

3.IV.4 Results and Discussion

In order to carry out valid measurements, the relative photoresponse

obtained at a certain bias voltage should be independent of the collection field.

In Fig. 3.IV.3 the relative photoresponse of PPV is plotted against the

collection field (E_{coll}) at $E_{appl}=0$. As expected, with increasing the collection

field, photoresponse increase and then tends to reach saturation. However, at collection fields exceeding 170 V/μm, it sharply increases. This behaviour, which was observed for both broad band and laser illumination, can be attributed to detrapping of deeply trapped electrons and/or change in material property at high electric fields. In current experiments, where applicable, E_{coll} was chosen as 150 V/μm.

The electric-field-induced fluorescent quenching and photoresponse obtained upon laser excitation and at E_{coll}=150 V/μm are plotted versus the applied electric field in Fig. 3.IV.4a and b. It should be mentioned that fluorescent quenching measured under laser and broad band illumination were identical, indicating that results are independent of the peak power of the light source. For the sake of brevity the results obtained under broad band illumination are not presented. As is seen, fluorescent quenching and photoresponse are both strongly field dependant, and furthermore, the quadratic dependence of ϕ on E_{appl} is clearly illustrated. At the highest applied field about 32% quenching is achieved and a positive slope with no sign of saturation is observed. It is noteworthy to mention that the zero field carrier

generation (non-zero value of the photoresponse at E_{appl}=0) shown in Fig. 3.IV.4b is mainly due to the collection field (E_{coll}=150 V/μm) applied to the sample after illumination, which causes the first excited singlet states (excitons) to dissociate into geminate electron-hole pairs. The presence of impurities has also been reported to increase zero field carrier generation in other materials such as perylene (Popovic 1985).

In Fig. 3.IV.4c fluorescent quenching is plotted against photoresponse; a linear correlation exists at high E_{appl} between the two quantities. From the slope (m=0.966) and the φ-intercept (i=-0.1412) of the best linear fit through the data obtained at high field, the correlation factor C can be determined by rewriting Eq. 3.IV.4 as

$$\phi(E) = \frac{C}{1-\eta_G(0)} R(E) - \frac{\eta_G(0)}{1-\eta_G(0)} \qquad (3.IV.6)$$

where $\eta_G(0)$ is the geminate e-h pair yield at E_{appl}=0. Using the slope and the intercept mentioned above, the proportionality constant is calculated as C=0.846 and the φ-η relationship can be expressed as,

$$\phi(E) \cdot 1.141 \eta(E) \cdot 0.141 \qquad\qquad (3.IV.7)$$

To obtain true quantum efficiency η, the photoresponse (PR) plotted in Fig. 3.IV.4b has been rescaled by incorporating the parameter C determined above, (see also Eq. 3.IV.3). As is seen, carrier generation efficiency of about 42% is achieved at E_{appl}=300 V/μm. The fluorescent quenching efficiency obtained here will be compared to the values reported in the literature later in the paper.

The experimental data depicted in Fig. 3.IV.4c clearly demonstrates that at high electric fields almost all field-quenched excitations lead to production of free carriers. The departure from linear response at low fields, which is attributed to $\Omega(E)<1$, shows that at low fields only a fraction of geminate pairs results in the formation of free carriers. This indicates that high electric fields are required for full dissociation of all geminate pairs. Therefore, it is concluded that carrier generation process in PPV occurs via two steps. In the first step geminate e-h pairs are created upon light

illumination, and then the bound e-h pairs dissociate into free carriers under high applied fields.

The experimental data presented in Fig. 3.IV.4c also shows that the collected charge at E_{app}=0 is about half of the value expected had the linear fit held for all applied electric fields. This observation, which has also been noted for other materials (Popovic 1984), signifies that only half of the photogenerated excitations dissociate at zero applied field. This could be due to energetics and orientation of the geminate e-h pairs. At low applied field there is not enough activation energy for chain-to-chain transfer of charge carriers, and the e-h pairs oriented in the opposite direction of the field are forced to recombine, while only the e-h pairs in the direction of the field dissociate into free carriers.

The dependence of relative photoresponse on collection delay time is demonstrated in Fig. 3.IV.5. With increasing the delay time between excitation and charge collection, the photogenerated e-h pairs have more time to recombine and, therefore, carrier generation efficiency decreases. The

lifetime of these carriers is less than a few μs (in agreement with the value reported by Lee), and a majority of them (about 70%) decay non-exponentially to ground state about 1ms after illumination. The non-exponential decay may be attributed to the presence of impurities and their interaction with charge carriers.

Time evolution of the photo-induced voltage at $E_{appl}=E_{coll}=150$ V/μm is depicted in Fig. 3.IV.6. It is evident that the charge collected during the first half cycle (NESA positive) is higher than the ones measured during the second half cycle (Au/Pd positive). This asymmetry, which is observed in many materials, can be explained in term of low mobility and/or trapping of electrons. Since the sample is illuminated from the NESA side, most of the e-h pairs are created in the PPV layer adjacent to the NESA electrode. Bearing in mind that electron mobility in PPV is less than hole mobility by 2 to 3 orders of magnitude, when NESA is negatively biased electrons will cross shorter distances (have shorter ranges) than holes when NESA is positively biased. Therefore, a larger response is obtained when NESA is positive, and holes are moving into the sample bulk. Time evolution data also indicates that about

42% of the total (averaged) photoresponse evolves in about 100ns and the rest emerges in 1ms. The fast rising part of this graph is attributed to the fast moving carriers (holes) and the slow rising part is believed to be due to the sluggish mobility of electrons.

3.IV.5 Conclusions

Strong electric field dependence of fluorescent quenching and photoresponse have been observed in PPV. The data demonstrates a linear correlation between fluorescent quenching and carrier generation efficiency at high applied fields, indicating that all of the photogenerated excitations lead to production of free carriers. It is also concluded that carrier generation process in PPV follows two steps; bound e-h pairs are generated upon excitation and then dissociate into free carries under applied electric field. Carrier generation efficiency of 42% was detected at E_{appl}=300 V/μm. Fluorescent quenching of up to 34% was achieved at E_{appl}=300 V/μm which decreases to 15% at 200 V/μm. This is lower than the value reported by Bassler. They report 30% quenching at E_{appl}=200 V/μm, twice the one obtained here. This discrepancy can be due to the differences in sample

preparation and thickness measurements. For example, in the current study the sample thickness was determined by taking the dielectric constant as $\epsilon=3$. However, dielectric constants of 4.3 and even 22 have also been reported (Reiss 1994 and Karg 1994) for PPV. Assuming, for example, $\epsilon=4$, the sample thickness can be recalculated as $d=2.867\mu m$, and by readjusting the applied field accordingly, about 29.7% fluorescent quenching is obtained at $E_{appl}=200$ V/μm, which agrees well with the value reported by Bassler.

(a)

(b)
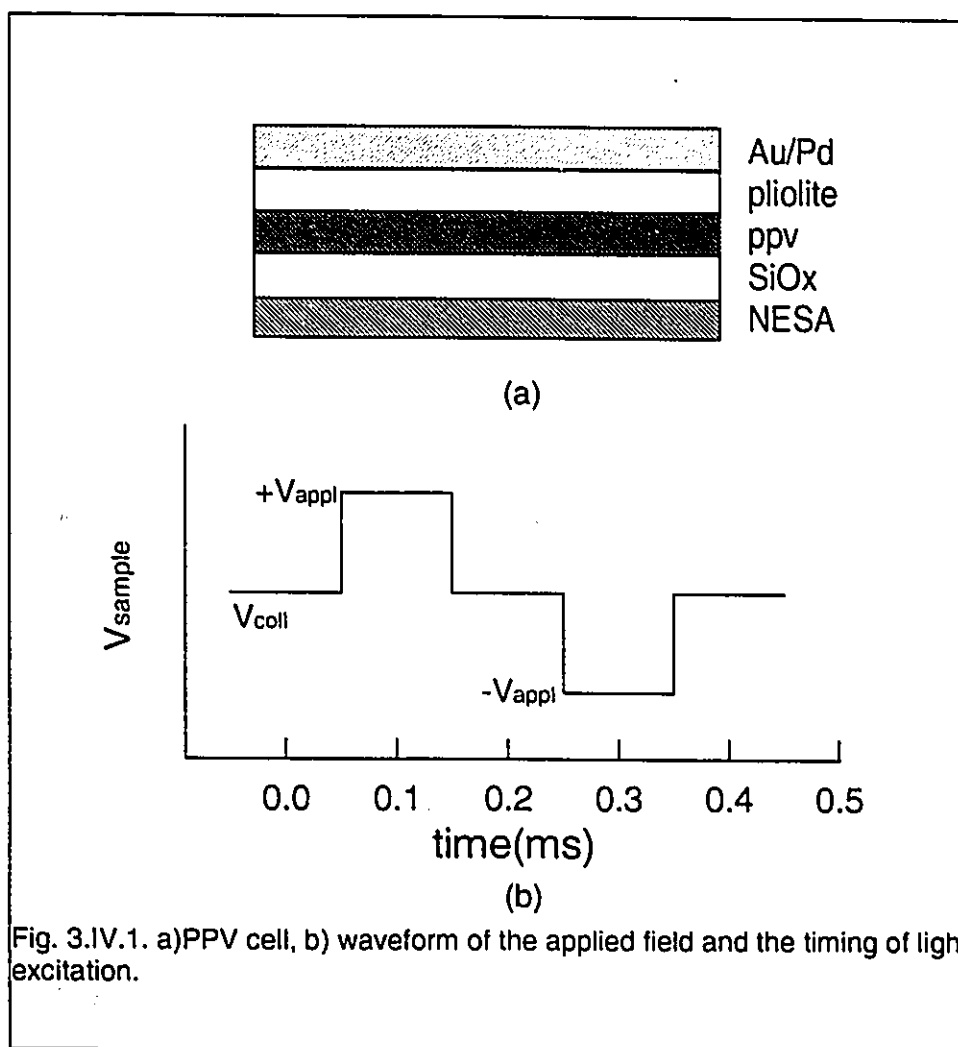
Fig. 3.IV.1. a)PPV cell, b) waveform of the applied field and the timing of light excitation.
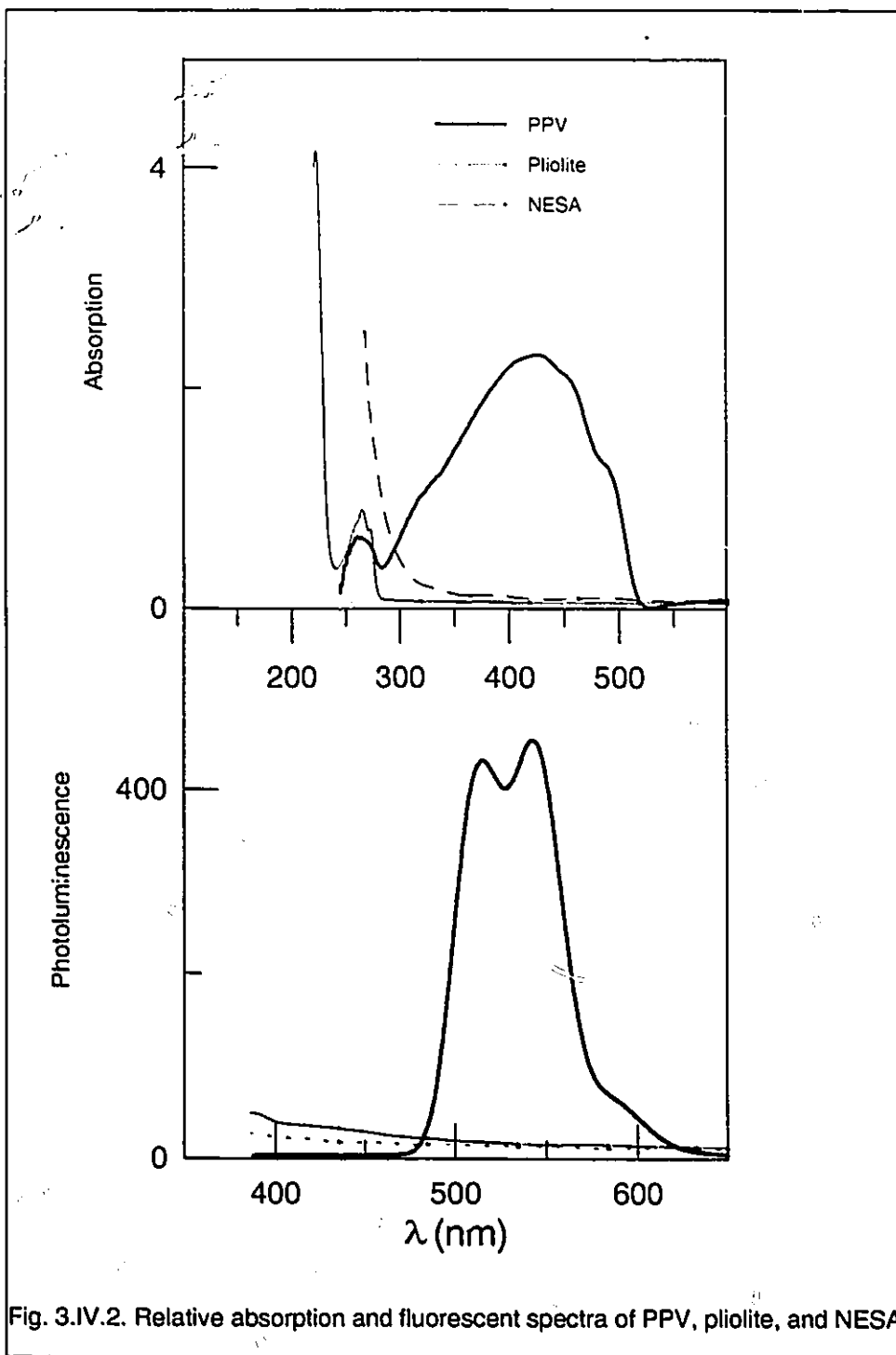
Fig. 3.IV.2. Relative absorption and fluorescent spectra of PPV, pliolite, and NESA.
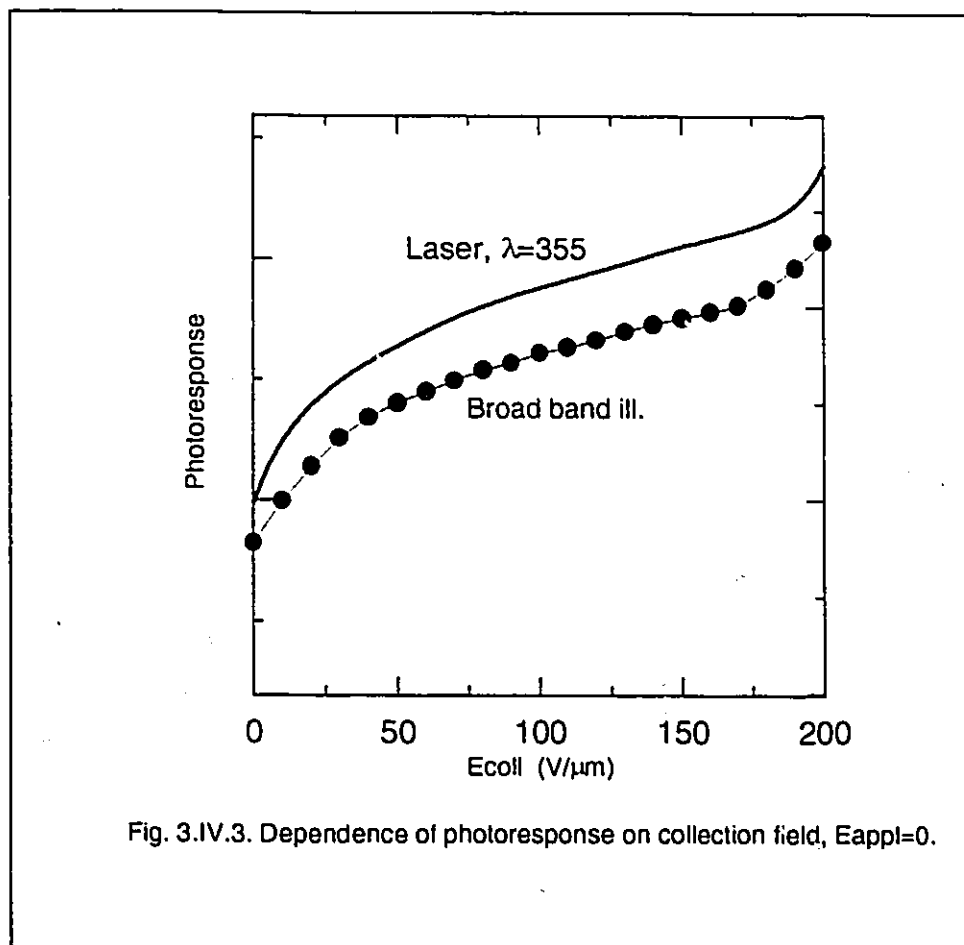
Fig. 3.IV.3. Dependence of photoresponse on collection field, Eappl=0.

Fig. 3. IV.4 . a)Fluorescent quenching versus applied electric field.
b) Photoresponse and normalized quantum efficiency versus apllied
filed. The scale for η was calculated by multiplying photoreponse by
the proportionality constant C=0.846.
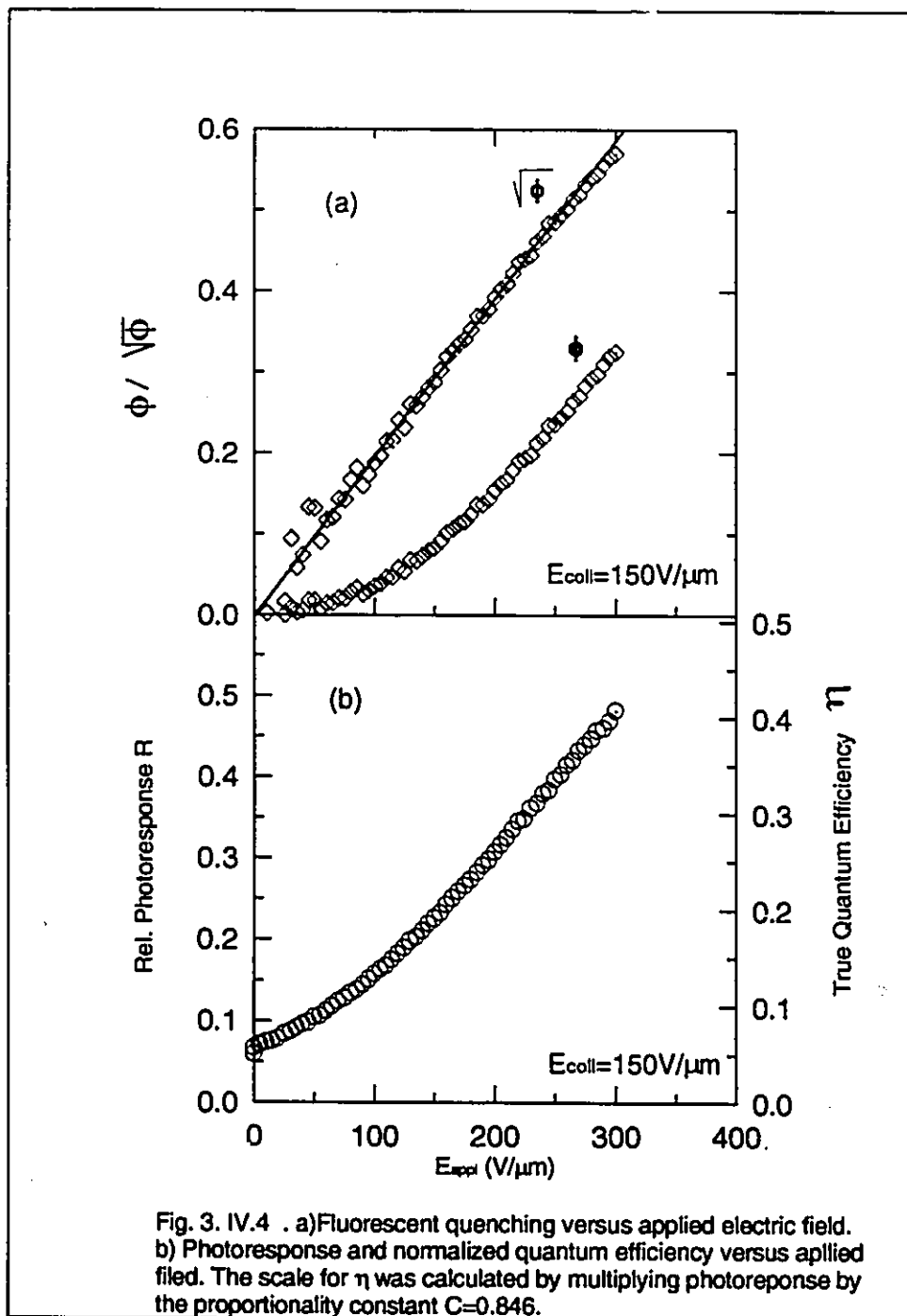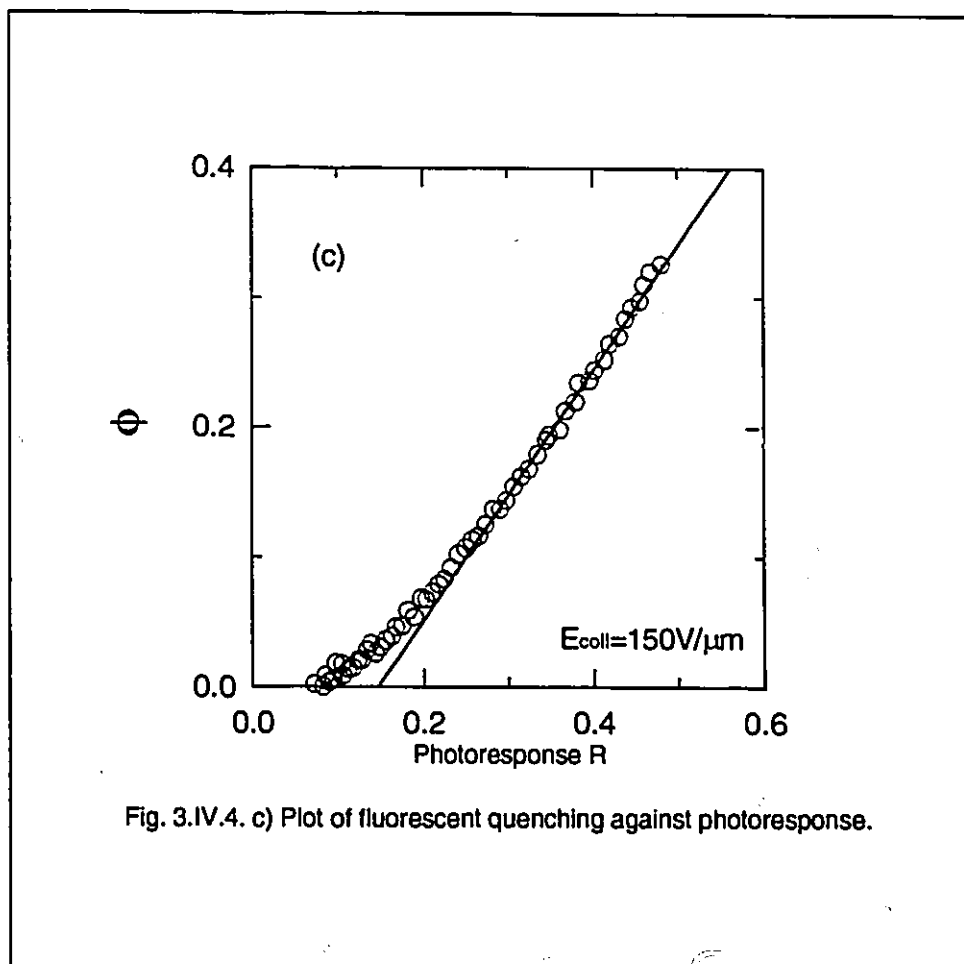
Fig. 3.IV.4. c) Plot of fluorescent quenching against photoresponse.

3.IV.5 Variation of relative photoresponse with the collection delay time.

Fig. 3.IV.6. Time evolution of the photo-induced voltage at Eappl=Ecoll=150V/μm.
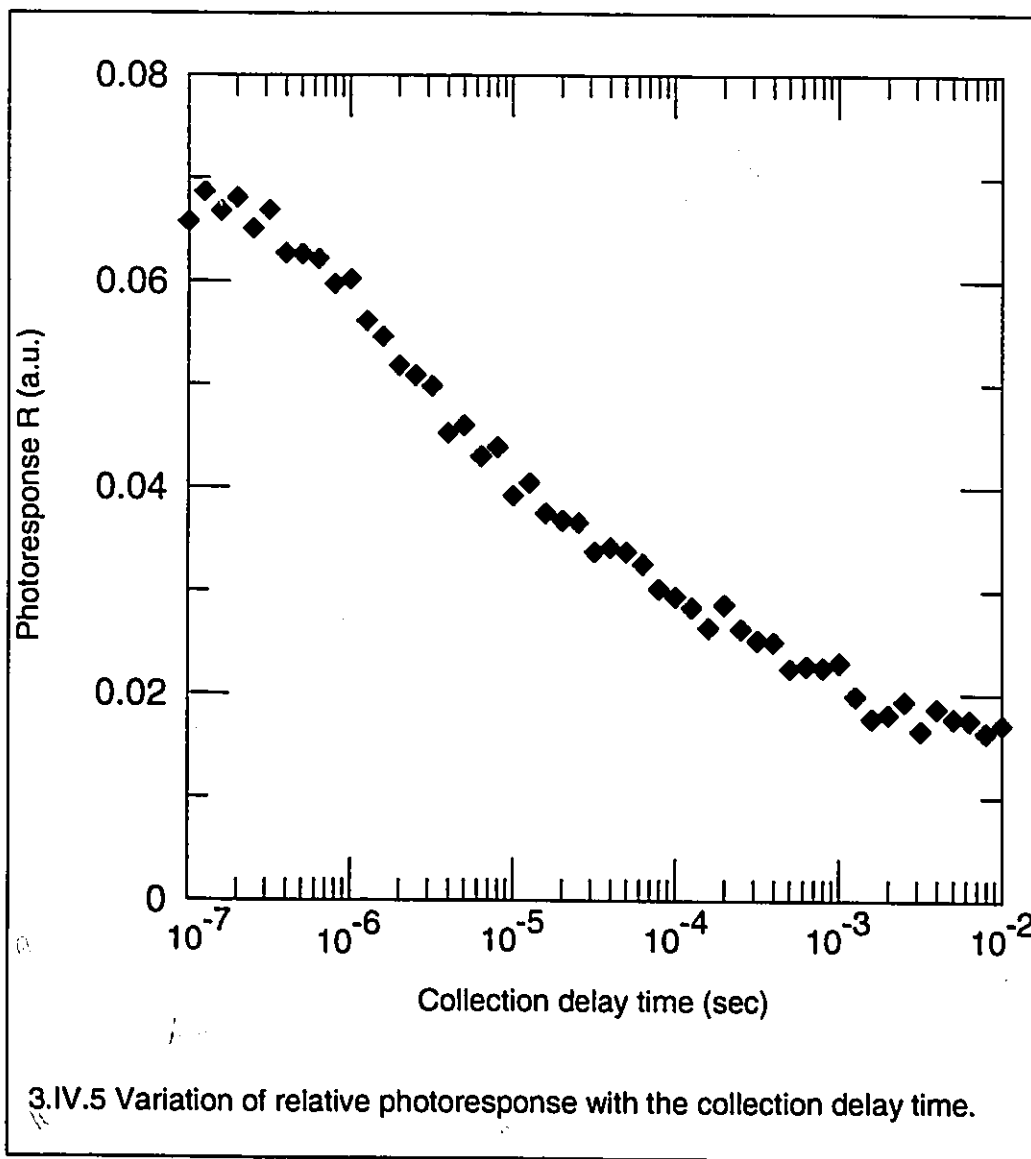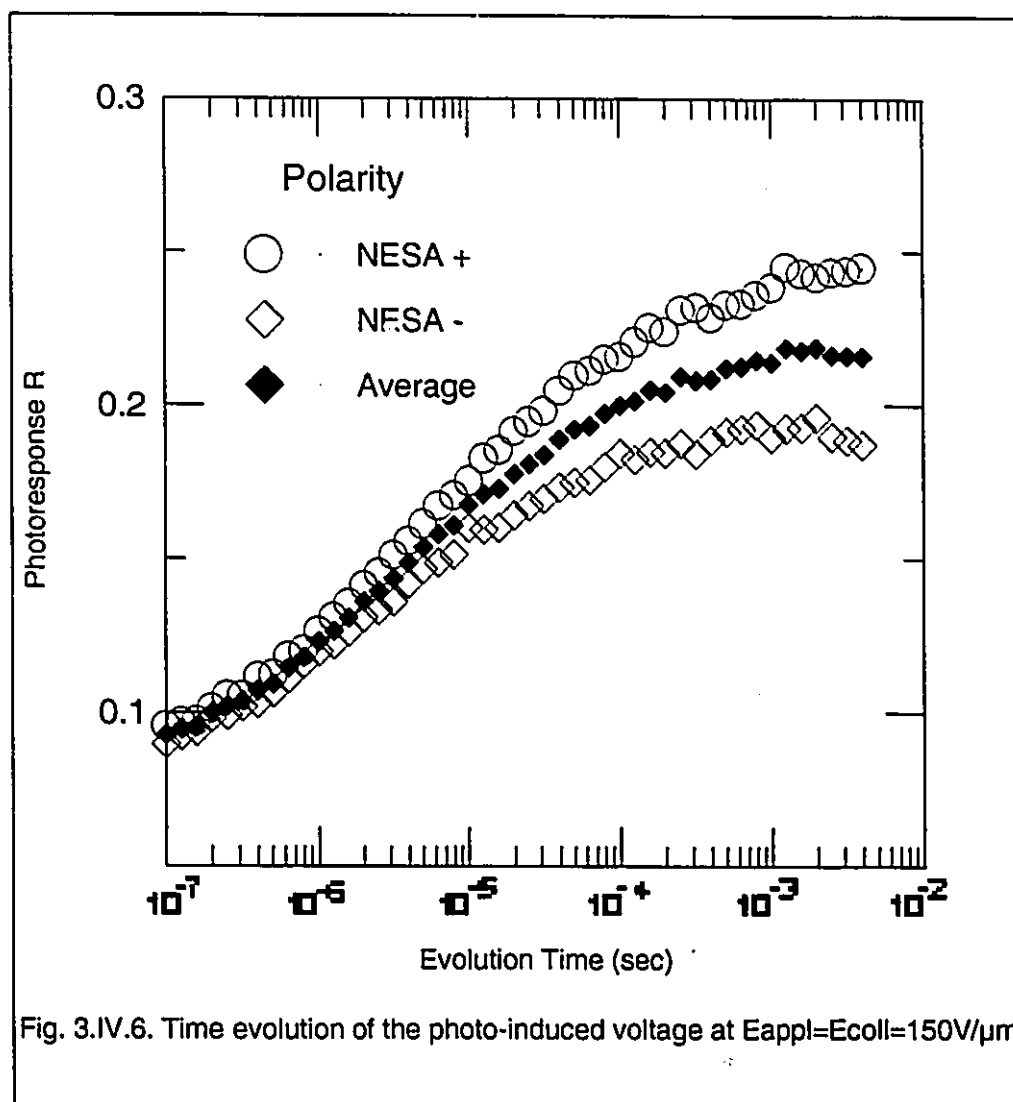
Chapter 4

Crystallinity in PPV

Several investigators have recently reported photo- and electro-luminescence enhancement by inducing (or increasing) disorder in PPV (Yan 1994 and Son 1995). This fact is claimed to be due to the decrease in the quenching centres with decreasing the crystallinity. Crystallinity and the formation of crystals in polymers depends on a number of factors among which the presence of trans-linkage on the polymer chains has been known to favour the formation of local order in polymers. Cis- or a mixture of cis- and trans-conformations lead to a less densely packed polymer and tends to result in the formation of a more amorphous material (Cowie 1991 and Young 1987). By taking advantage of this fact and using a different approach in the synthesis of PPV, Son *et al.* (1995) claimed to have introduced cis-segments onto PPV chains and were able to decrease the amount of trans-linkage and thus decrease crystallinity. They also claimed that their film was completely amorphous and reported a significant increase in electroluminescent quantum efficiency; from

0.01% reported by Burroughes to 0.22%, an increase of approximately 20 times.

The aim of the present chapter is not to dispute the inverse relationship between crystallinity and luminescent yield, but rather to examine PPV structure and address the cause of the formation of these crystals, and also to compare quality of the films prepared by the author with the onees prepared by the group mentioned above. It is believed that a thorough investigation of PPV morphology is fundamental in preparing high quality amorphous films with high quantum yields.

Transmission electron microscopy (TEM) was used to examine PPV structure and morphology. In TEM electrons emitted from an electron source are accelerated by a high potential, and via a series of magnetic lenses are focused onto the specimen. The diffracted or transmitted beam are then magnified by three or more lenses to form the image or a diffracted pattern. In the convergent beam diffraction (CBD) technique, which was employed here, portions of the specimen as small as 0.5 nm in diameter can be scanned with a highly convergent beam, and useful information about lattice constants and

crystal structures can be obtained. A beam energy of 120 KeV was used and

cautions were exercised to prevent polymer degradation (due to the exposure

to the elecron beam) during examination. Thin films of PPV with thickness of

d=33 nm were prepared by the method explained in Chapter 2.

A CM12 TEM was used in imaging mode to obtain the micrographs

shown in Figs. 4.1 and 4.2. These micrographs illustrate PPV morphology at

40,000 and 260,000 magnifications. Visual examination of the pictures

indicates that aggregates of crystals are embedded in an amorphous matrix. In

order to further investigate these crystals, the convergent beam diffraction

method with a convergence angle of 2.7 mrad was used. The diffraction

patterns of the crystals are depicted in Figs. 4.3 and 4. By analysing the

diffracted spots, an average lattice parameter of a=0.292 nm was calculated.

A diffracted ring pattern was also obtained as depicted in Fig. 4.5. The rings

were indexed by measuring their diameters and calculating the ratio of the

squared diameters to that of the first ring, as tabulated in Table 4.1. With the

exception of ring number 2 and 9, the mixed indices indicate that the pattern

is from an FCC structure.

A careful examination of the experimental facts presented here strongly suggests that the crystals under consideration are not PPV crystals. The reasons are as follows.

1) Considering that the size of a simple PPV monomer is at least 0.6 nm, the lattice constant is too small for a PPV unit cell.

2) It is very unlikely for PPV to have a FCC structure. This speculation is made due to the fact that simple polymeric materials such as polyethylene or polyacetylene have orthorhombic crystal structures, and it seems unrealistic that PPV crystals are FCC.

Further investigation of the samples by electron energy loss spectroscopy (EELS) revealed that these crystals are in fact NaCl crystals. The presence of NaCl originates from the addition of sodium hydroxide as the initiator and hydrochloric acid as the terminator to the polymerization reaction. Due to insufficient purification NaCl precipitates during casting, and forms small colonies of crystals and/or acts as nuclei for PPV crystallization. In fact the presence of ring number 2 and 9 is thought to be due to the nucleation and

growth of PPV crystals on these seeds.

By removing impurities, salt-free PPV films were prepared which were amorphous and showed little or no crystallinity. Therefore, it is believed that minute amounts of NaCl present in the solution act as seeds upon which PPV crystal are nucleated and grown, leading to small scale local orders. Furthermore, the PPV crystallinity mentioned by (e.g.) Son *et al*. might be due to the presence of impurities and their elimination would lead to an amorphous structure and the use of new synthesis method might not necessarily result in a more amorphous material, as explained below.

Two IR spectra, one from a PPV film prepared by the synthesis method suggested by Son *et al*. and one from a film prepared by the author, are compared in Fig. 4.6. The peaks at 962 cm^{-1} and 868 cm^{-1} respectively represent the formations of trans- and cis-conformations, as indicated on the graph, (for a complete peak assignments see Bradley 1987-a). The IR spectra of Fig. 4.6.a suggest that with increasing the conversion temperature the ratio of the cis to trans content of PPV first increases and then decreases, and the final content of cis-PPV is much less than the amount of trans-PPV. Fig. 4.6.b,

on the other hand, reveals that this ratio stays relatively constant once the conversion temperature exceeds 150 °C, and the final amounts of cis- and trans-PPV are almost equal. The conclusion which can be drawn from all these is that, if the amount of cis-linkages present in the polymer is taken as the degree of amorphousness, the synthesis route put forward by Son *et al.* has definitely not resulted in a more amorphous material. Furthermore, the synthesis method utilized here has produced a polymer with a higher content of cis-linkages and is more amorphous, and therefore has a better quality. The higher quantum yield obtained by the author (0.59%), compared to 0.22% reported by Son, is a clear indication of the better quality PPV films prepared by the author. Note that the 0.59% yield mentioned above is a conservative figure and still higher yields are expected, as explained in Chapter 5.

Fig. 4.1 Electron micrograph of a PPV film at 40,000 X.

Fig. 4.2 Electron micrograph of a PPV film at 260,000 X.
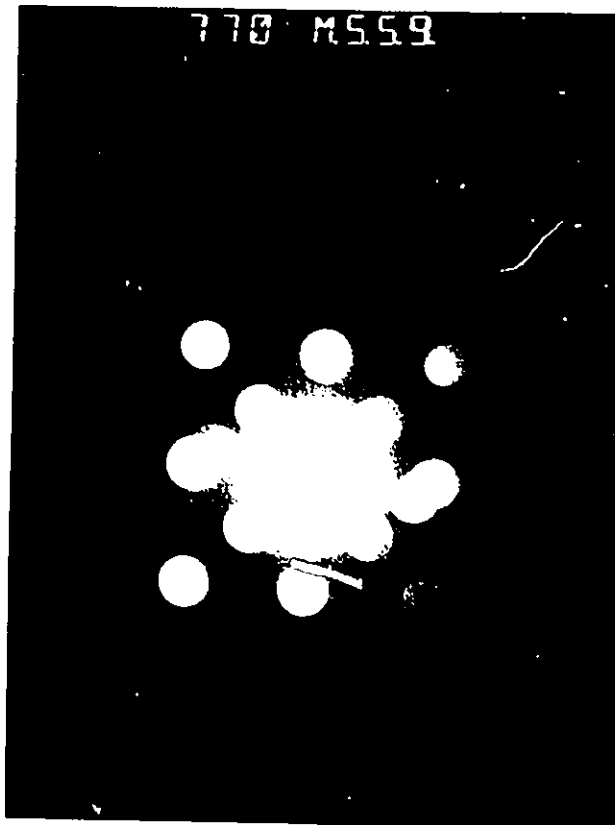
Fig. 4.3 Diffraction spots pattern along <001> direction.
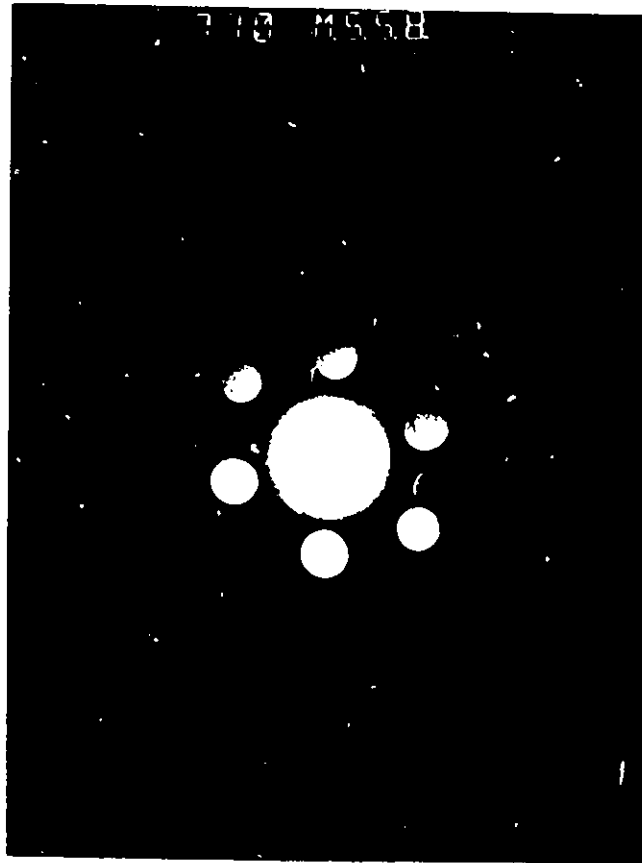
Fig. 4.4 Diffraction spot pattern along <0,1,-1> direction.

Ringe	Diameter (mm)	D^2/D^2	h k l
1	21.0	1.00	1 0 0
2	25.5	1.48	
3	29.5	1.97	1 1 0
4	36.5	3.02	1 1 1
5	42.0	4.00	2 0 0
6	46.5	4.90	2 1 0
7	49.0	5.40	2 1 0
8	51	5.90	2 1 1
9	55.5	7.00	
10	59.5	8.02	2 2 0
11	64.5	9.43	2 2 1

Table 4.1. Diffraction indices of the ring pattern shown in Fig. 4.5

Fig. 4.5. Diffraction ring pattern of the crystals shown in Fig. 4.1 & 4.2.
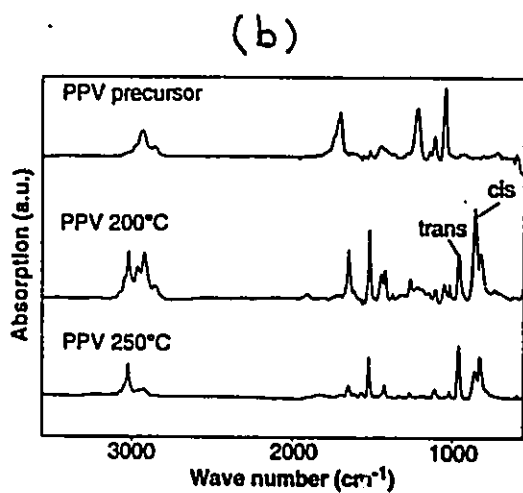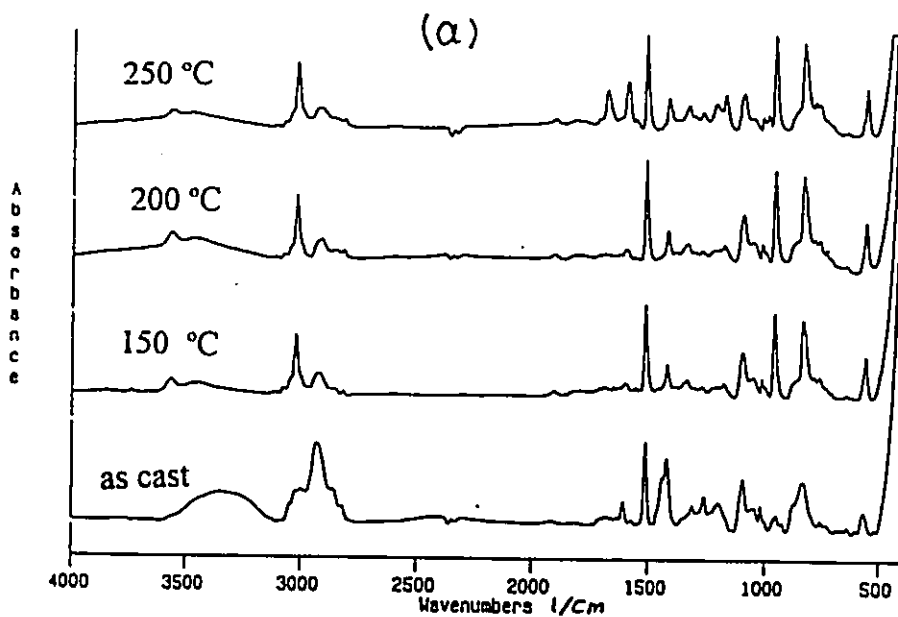
Fig. 4.6 Comparison of IR spectra of PPV at various temperatures.
a) present work, b) work of Son *et al*.

Chapter 5

Electroluminescent Devices;

Fabrication and Characterization

5.1 Fabrication

As was mentioned in the experimental section, EL devices are fabricated by casting or spin coating the precursor polymer onto ITO-coated glass substrates. Prior to casting, narrow strips of ITO were etched out on the substrates by using a solution containing HCl/HNO_3 as an etchant. After the eli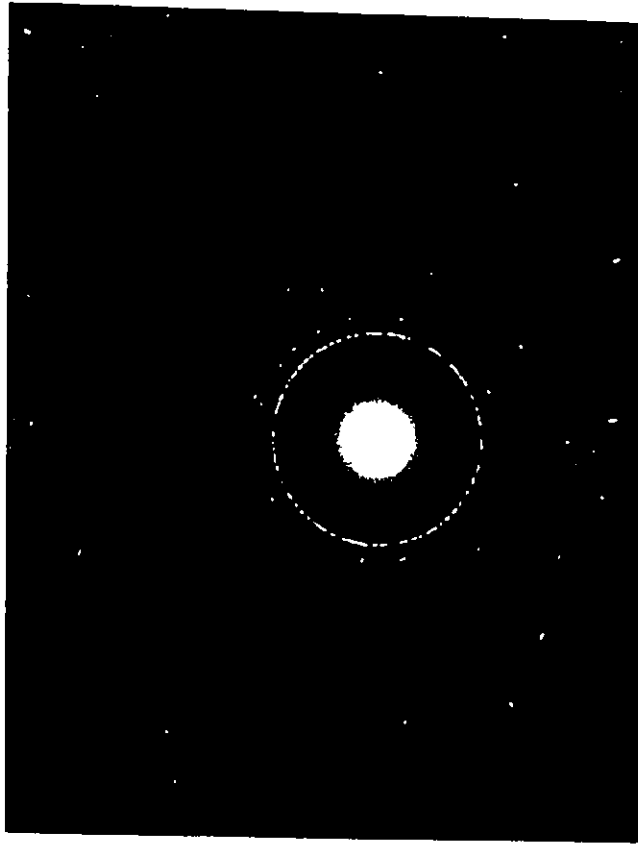mination process the top electrode (Al) was vacuum-evaporated onto the sample in the form of narrow strips at right angle to the ITO strips. A schematic diagram of a typical ELD is drawn in Fig. 5.1. The width of Al or ITO strip varied from 1 mm to 6.35 mm, which produced an effective area of 1 to 40 mm². After connecting the top and bottom electrodes to a DC power supply, current-voltage (I-V) characteristics of these cells were measured. Typical I-V curves and the thresholds of electroluminescence are illustrated in Fig. 5.2. In general, when measuring I-V and EL characteristics of these

diodes it was observed that, i) the diodes were extremely unstable and the results were practically not reproducible, ii) only a small percentage of these devices could emit light and, iii) the light intensity was very low and the emitted light was short-lived. Attempts to conduct the measurements under a metallic shield to reduce noise and/or under a protective atmosphere to exclude oxygen/moisture did not significantly improve the reliability of the data. To address these issues a careful examination of the entire process, from the synthesis stage to the device preparation was required. Following is a detailed investigation of the problems leading to device failure.

a) Synthesis

Two areas of device failure and instability, which were traced to the synthesis process, are the presence of pinholes and the corrosion of ITO electrode. The presence of pinholes is closely related to the quality of the precursor solution and the difficulties encountered during solution casting. The precursor solutions which were prepared at polymerization temperatures higher that 0 °C (due to careless control of the polymerization conditions) resulted in the formation of short chains, presence of which reduced the viscosity of the solution. Consequently, the solution would not spread evenly

over the substrate leading to the formation of pinholes. This problem was rectified by carefully controlling the reaction temperature and by using dialysis tubes with MWCO of 12000 to 14000 Dalton instead of 3500 Dalton. This greatly improved solution casting of thin uniform films having thicknesses as low as 30 nm. While retaining longer chains, tubes with larger pore size allow the shorter chains to diffuse out of the solution, thus enhancing film casting and quality.

Another cause of device failure is believed to be due to the presence of HCl in the precursor solution. Hydrochloric acid is added to the precursor solution to terminate the polymerization reaction and if sufficient purification is not carried out it reacts with ITO and destroys the bottom electrode. The reaction of HCl with ITO can take place during casting and conversion process and/or during device characterization. The latter is more severe, because the reaction of HCl with ITO is accelerated in an applied electric field. This was confirmed by measuring the resistance of ITO strips in Al/PPV/ITO diodes. It was noticed that in some devices after a DC voltage was applied for a short time ($\approx$20 minutes), no current would pass through ITO electrodes; ITO showed infinite resistance. Since ITO can be corroded in both acidic and basic

environments (Handbook of Chemistry and Physics, CRC 1990), in order to protect ITO electrodes the addition of HCl to the basic precursor solution was performed in such a way to bring the overall pH of the solution to ≈6.8-7. Using a neutral solution almost entirely eliminates the corrosion of ITO electrodes.

b) Elimination Conditions; Temperature, Time and Atmosphere

After casting and drying PPV films, they are heated to relatively high temperatures. This is to remove the thiophenium side group and convert the precursor solution to PPV. Although the conversion process starts at about 160°C, in order to achieve full conversion, temperatures higher than 300°C has been suggested (Bradley 1987). However, it was observed that increasing the elimination temperature substantially reduces the PL intensity (Esteghamatian 1994-b). In Fig. 5.3 the photoluminescence intensity of PPV films eliminated at various temperatures is plotted versus wavelength of the emitted light. As is seen, the PL intensity considerably decreases with increasing the elimination temperature. The exact cause for this phenomenon is not well understood, however, it is attempted to provide some explanation, as follows.

Increasing the elimination temperature facilitates the removal of thiophenium side group and has a bathochromic effect on the PL spectra. In Fig. 5.4 PPV band gap is plotted at various stages of elimination. As illustrated, with increasing the temperature E_g decreases, indicating an increase in the extent of conjugation length. Increasing the π-electron delocalization allows more rapid motion of photo-excited carries to the quenching sites, which results in non-radiative recombination of the e-h pairs. These quenching sites or defects are formed basically by the reaction of PPV with oxygen. Due to an insufficient vacuum, after the removal of thiophenium group oxygen reacts with carbon on the vinylene part of PPV to from C=O. The presence of an absorption peak in IR spectrum of PPV at 1690 cm^{-1} substantiate the formation of carbonyl groups on the main chain (see Fig. 3.I.1). This was also confirmed by Yan (1994), who experimentally demonstrated an inverse relationship between PL and the percentage of oxygen in PPV.

From the results and argument presented above it was concluded that high quality PPV films should be prepared under the conditions that made the conversion of PPV at low temperatures possible and prevented oxygen from reacting with the polymer and forming carbonyl groups. Attempts to process

PPV at a lower temperature under a higher vacuum or under a flow of nitrogen gas were unsuccessful; it required a lengthy processing time which was not practical and did not produce better quality films. However, elimination under a gentle flow argon gas proved to be highly successful. Not only did it substantially reduce reaction of oxygen with PPV, but also it dramatically lowered the elimination temperature and duration. In Fig. 5.5 the UV-visible absorption and PL spectra of PPV films converted under vacuum and argon are presented. It is clearly observed that, conversion of PPV can be achieved at lower temperatures under an argon atmosphere. Also, note the duration time which is reduced from 12 to 24 hours under vacuum at 300°C to 2-4 hours under argon at 160°C. Argon is thought to have a kinetic effect on the elimination process. Due to its larger mass, argon quickly removes from PPV surface the elimination products whose bonds with the main chain have already been weakened or broken, thus creating a sharp concentration gradient of the elimination product through the PPV film which further facilitates the conversion process.

The reaction of PPV with oxygen was examined by employing impedance spectroscopy. This technique is widely used in many areas of

research and can provide useful and important information about the electrical

properties of polymer cells. This is the first time, however, that this technique

has been applied in probing the interface properties of a polymer LED. In

general, the response of a polymer system to an AC signal is modelled by

using an equivalent circuit of electrical components, usually made of

capacitors and resistors. These components are then related to the actual

physical properties of the system by using the experimental data (Bruce 1987).

The oxidation of PPV results in the formation of an interface layer between

PPV and Al, which can be detected by this technique. The presence of an extra

semi-circle on the cole-cole plot indicates the formation of the interface layer.

Impedance measurement made on PPV films which were converted under

vacuum or under argon are plotted in Fig. 5.6. The absence of the second

semi-circle on the impedance plot of the argon-converted PPV films clearly

indicates that argon eliminated to a great extent the reaction of oxygen with the

PPV surface onto which Al or Mg would be deposited as the top electrode.

The substantial decrease in the threshold voltage (V_{th}) of electroluminescence

can also be partially attributed to the use of argon and the absence of a PPV/Al

interface. This interface is believed to create a space charge and hinder charge

transfer from Al to PPV, and consequently increase the drive voltage in the

ELD's.

In general, devices made under argon were much brighter, more stable and longer-lived, which enabled the author to measure the diode characteristics of these devices with a great improvement in reproducibility, as presented below.

5.2 Electroluminescent Device Characterization

After addressing the problems discussed above, EL devices were fabricated and characterized. In Fig. 5.7 the I-V behaviour of the PPV ELD's prepared under argon are presented. A comparison of this figure with Fig. 5.2 demonstrates that a significant improvement has been achieved in lowering V_{th}. The V_{th} obtained here is also lower than the values reported previously; $V_{th}=13.5V$ (Burroughes 1990), and $V_{th}=12V$ (Hu 1994). Since these devices operate under a constant DC voltage, heating of the device due to the internal resistance (Joule effect), which leads to local heating and degradation of the polymer film, is expected. Therefore, by lowering the drive voltage the performance and lifetime of these devices can be improved. Also, note that the slope of the I-V curves, which represents the inverse of internal resistance

(1/R), is relatively higher for the argon-converted samples compared to vacuum-converted samples shown in Fig. 5.2. The decrease in the internal resistance reduces the Joule effect and can enhance device performance.

A typical electroluminescent spectrum of an Mg/PPV/ITO diode, measured under ambient conditions, is depicted in Fig. 5.8. The colour of the emitted light which could be seen under normal laboratory lighting is greenish yellow and the emission spectrum ranges from 500 to 650 nm. The PL and EL spectra look more or less identical which suggests that the same mechanism leads to light emission. EL occurs when electrons and holes are injected from Al and ITO electrodes respectively into the sample. These charge carriers form electron-hole pairs, which can recombine radiatively and release photons. Devices made with Mg as the electron injecting electrode improved the intensity and the overall device performance. This is mainly because Mg has a lower work function (Φ=3.7eV) than Al (Φ=4.3eV) which facilitates electron injection into the sample. It should, however, be mentioned that some of the devices made with Mg performed poorer than the ones made with Al. This is because Mg is highly reactive with oxygen and careless handling or insufficient vacuum during electrode deposition would lead to oxidation of Mg

which consequently results in the formation of an oxide layer between Mg and PPV. The presence of an oxide layer in the ELD structure would require a higher drive voltage which may cause the breakdown of the cell.

The EL-V and I-V characteristics of a Mg/PPV/Al device are plotted in Fig. 5.9.a. The threshold of electro-luminescence is about 4V, however, depending on the elimination conditions, PPV thickness and the electron injecting electrode, threshold voltages as low as 2 V were attained. The first sign of visible light was detected at about 0.2 mA/cm^2 and the emitted light was uniform over an area of approximately 40 mm^2. In Fig. 5.9.b the device luminance is plotted versus the current density. The linear correlation between light output and the input power suggests that carrier injection limits the light emission. At higher current densities (J > 45 mA/cm^2) emission of light seems to reach a plateau indicating that other limiting factors are controlling the emission of light. These factors may include polymer oxidation and polymer break down under high bias voltage.

The efficiency of these devices varied over a wide range. A typical external efficiency of 0.4 Lumens/Watt (at V=8 volts) was measured. Since

almost all values reported in the literature are for the internal efficiency, in order to make a comparison, the above value should be converted into the internal efficiency of the device. The internal efficiency (the efficiency of the light emitted within the film) of this class of devices are always higher than the external efficiency which represents the light reaching the eye. The internal quantum efficiency was calculated with assumptions set forth by Greenham *et al.* 1994. The light emission from the OLED's was assumed to be Lambertian. In a Lambertian emission, also known as Lambert's cosine law, the flux per solid angle decreases symmetrically on all sides in proportion with the cosine of the angle from the normal. Also, the brightness of a Lambertian source is independent of the radiation source. The Lambertian emission has been in fact detected (to a good approximation) by the group mentioned above. It is also assumed that the negative electrode is perfectly reflecting and that the Al, PPV, and ITO layers are uniform and do not alter the angle of emission of light exiting the device, and thus, only the refractive index of the PPV layer is considered in these approximations. The light output was measured in the forward direction by a fibre optic detector positioned about 45 mm from the source.

By taking the refractive index of PPV as 1.6, the internal efficiency was calculated as $\eta=0.59\%$. The efficiency reported here for a single layer device is considerably higher than the value previously reported by Burroughes *et al* (0.01%), or by Son *et al* (0.22%). It is believed that this figure is an underestimate due to the fact that the Al or Mg contacts were not perfectly reflecting and that the emitted light could be clearly seen through the Al (Mg) contact. Therefore, a significant percentage of the light does not reach the detector and is lost through the back side.

The low efficiency in these diodes, however, can be attributed to several factors as follows.

1) As was mentioned before injection of charge carriers into PPV limits the light output. This limitation arises due to the high work function (Φ) of the electron injecting electrode and due to the presence of an interface (oxide) layer which increase the drive voltage required to render these devices luminescent. By using metals with a low work function, for example Ca with $\Phi=2.7\text{-}3.0$ eV, the efficiency can be improved. However, since Ca is highly reactive with oxygen, devices made with this metal should be fabricated and operated under a well protected atmosphere, which may not be practical.

2) Another major cause of low efficiency is the recombination of e-h pairs at the PPV/Al (or PPV/Mg) interface. PPV is reported to be a hole transporting polymer and the mobility of electrons in PPV is a few orders of magnitude less than the hole mobility (Bradley 1987-b). Due to sluggish movement of electrons in PPV, some of the e-h recombination may occur at the interface. The radiative and non-radiative recombination of these e-h pairs results in local heating and damage to the polymer film. Furthermore, since the EL measurements are made through the transparent electrode (ITO), the photons produced at the PPV/Al interface may be absorbed or refracted by the polymer film before reaching the detector, thus lowering the efficiency.

The lifetime of the best device measured here was just over a week, as presented in Fig. 5.10. The emitted light decayed to 60% of its maximum value in a short time but stayed steady afterwards. The lifetime of these devices were measured at room temperature and in air, and the short lifetime in PPV diodes are attributed to the reaction of oxygen and moisture with the device. Some investigators have claimed longer lifetimes for their multi layer devices by conducting the measurements under a protective atmosphere such as argon. However, for the single layer devices under consideration, the author did not

detect a significant improvement in either lifetime or light intensity by using

argon during measurements or by device encapsulation. Therefore, it is

speculated that the moisture absorbed during device preparation could be the

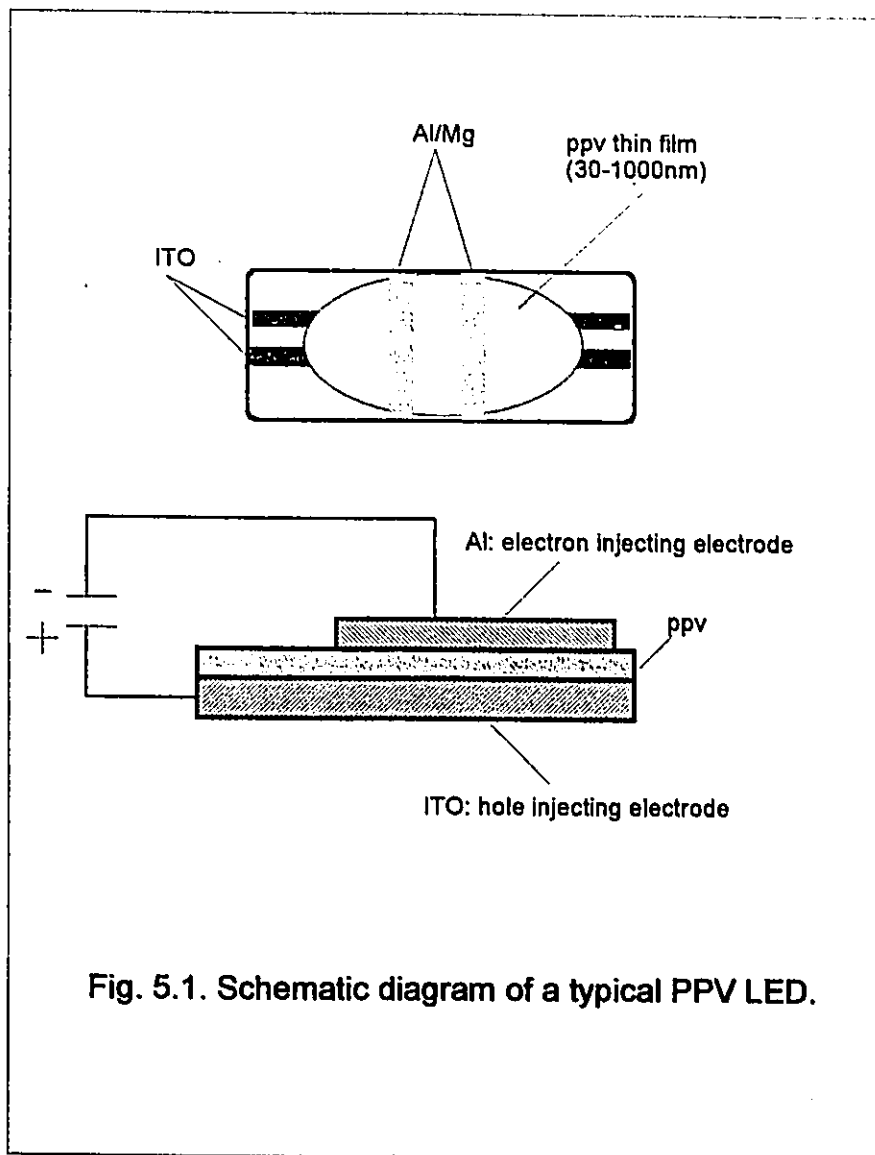cause for the short lifetime and device failure.

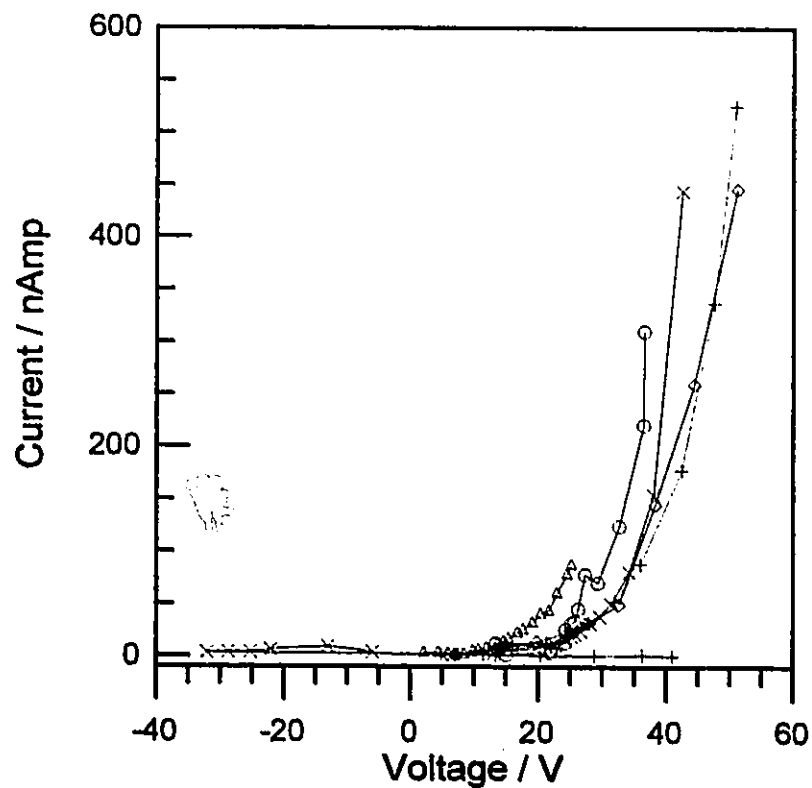Fig. 5.1. Schematic diagram of a typical PPV LED.

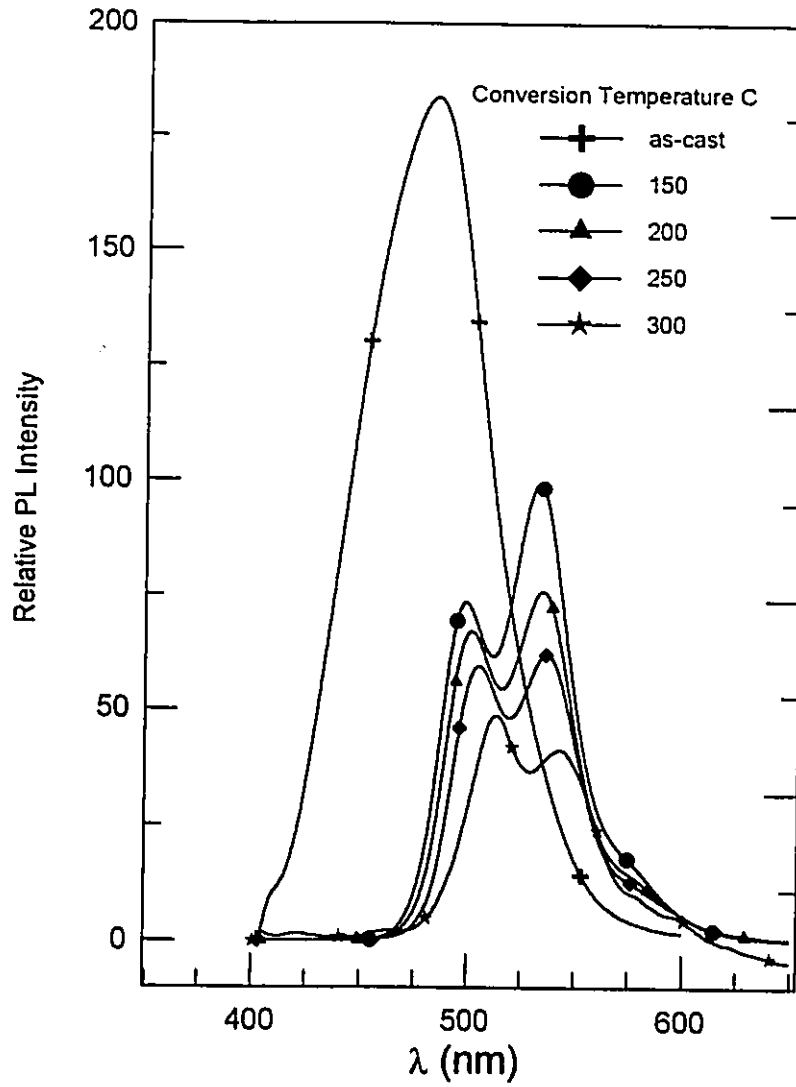Fig. 5.2. Current-voltage behaviour of some Al/PPV/ITO diodes converted in vacuum.

Fig. 5.3. Effect of conversion temperature on PL intensity. Increasing elimination temperature red-shifts PL spectra and substantially reduces fluorescent intensity.
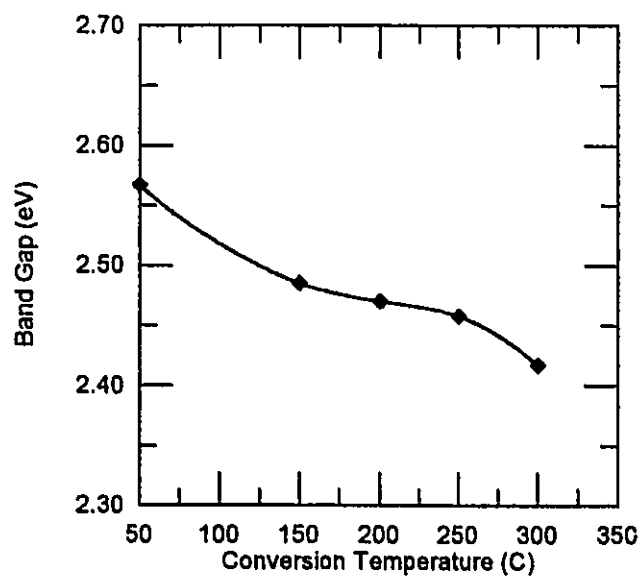
Fig. 5.4. PPV band gap as a function of el imination temperature.
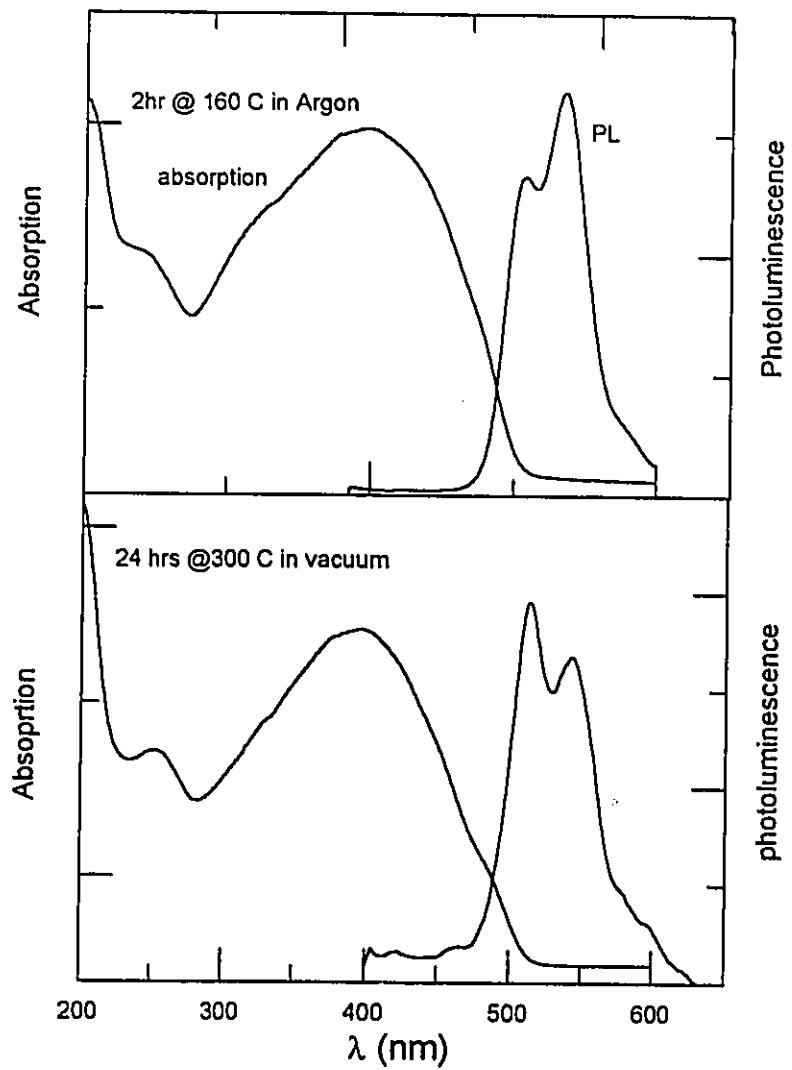
Fi g. 5.5. Effect of elimination conditions on optical properties of PPV.
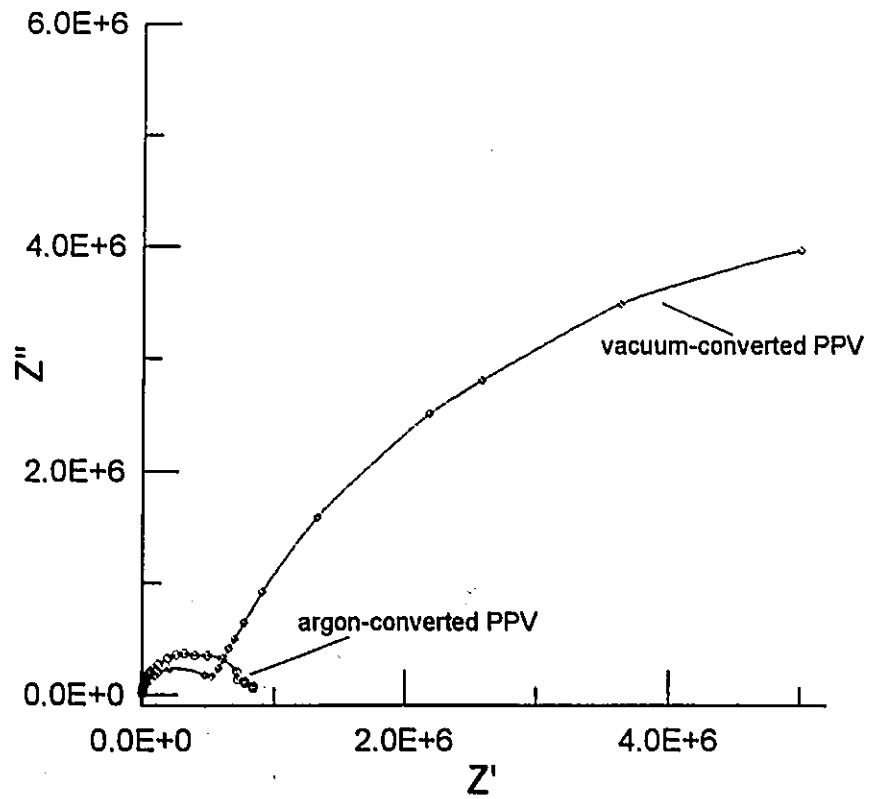
Fig. 5.6. Comparison of impedance plots of PPV converted under vacuum and argon.
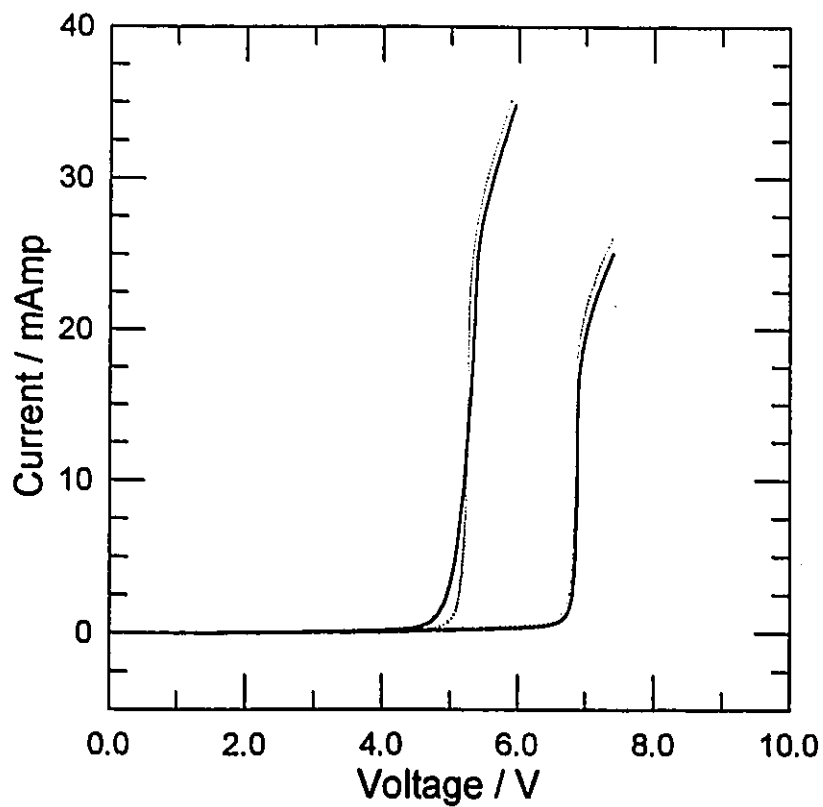
Fig. 5.7. Plots of current versus voltage of Mg/PPV/ITO diodes prepared under argon. Each set of curves represents measurements taken from a different diode. The reproducibilty of the data can be clearly seen.
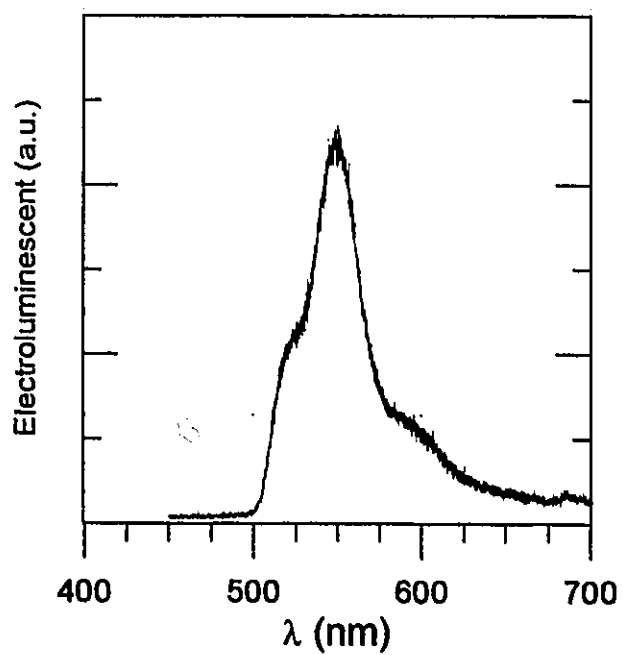
Fig. 5.8. The electroluminscent spectrum of PPV measured in air and at room temperature.
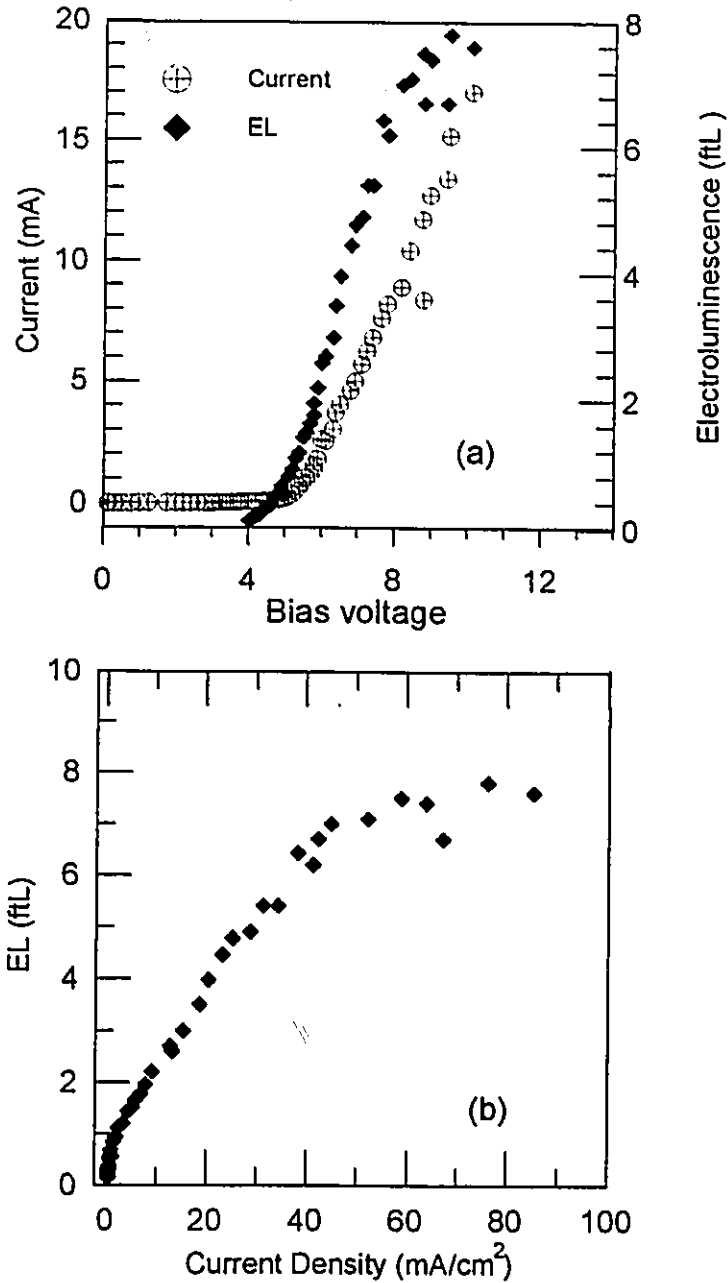
Fig. 5.9. a) Current and EL of a PPV diode versus applied voltage.
b) EL of the diode replotted as a function of current density.
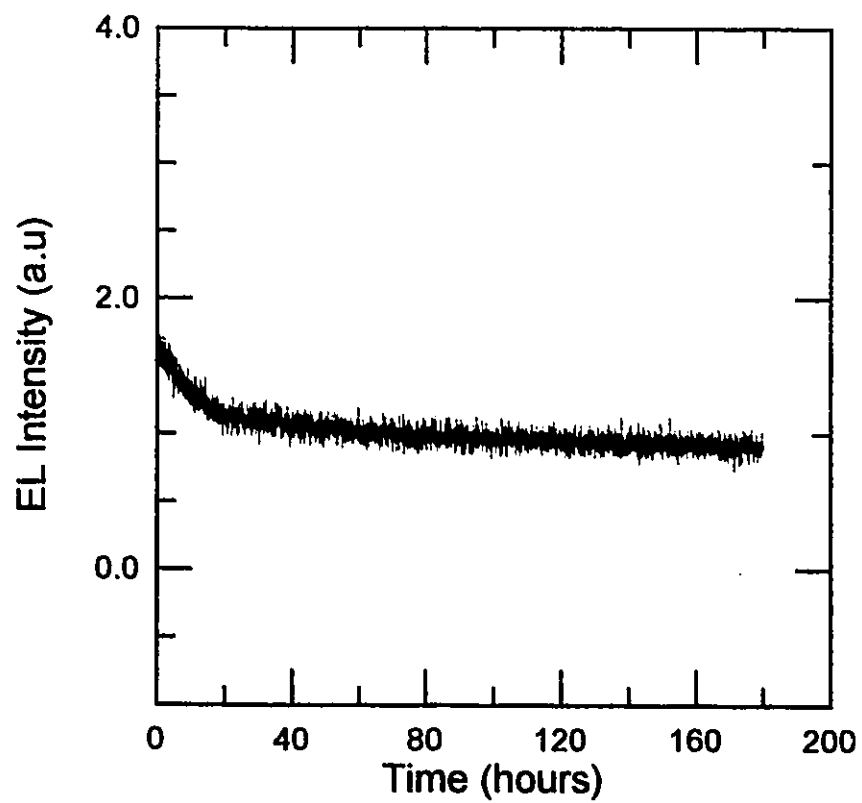
Fig. 5.10. Electro-luminescent lifetime of a PPV diode.

Chapter 6

Summary, Conclusions &

Recommended Future Work

6.1 Summary and Conclusions

In this thesis attempts were made to address some of the issues in preparing organic light emitting devices made from a conjugated polymer. While PPV was used as the primary material, some of the discussions and conclusions can be further extended to provide insight into other conjugated polymers currently exploited for OLED applications. These problems were basically classified into two groups. The first group included the problems related to the material preparation; i.e. polymer synthesis, elimination process and etc. The second group comprised of the issues encountered in device fabrication. Following is a summary and conclusion of these two parts.

PPV is one of the most promising candidate for EL devices. This

polymer was synthesized via the precursor route, which results in a polymer solution ready for film casting. The problems with film casting were overcome by introducing some modifications into the synthesis process. By using dialysis tubes with MWCO = 12000 to 14000 Dalton, oligomeric components and impurities were filtered out and a polymer solution with a high molecular weight was obtained. This significantly improved the film casting and films as thin as 30 nm were spin-cast with no apparent pinholes.

Compared with diffusion-doping, solution-mixing was found to be a much more effective method of doping PPV with lithium triflate. Upon doping with lithium triflate, the PL spectrum of PPV was red-shifted, indicating an increase in the number of charge carriers having sub-gap energies. This was confirmed by the 4 orders of magnitude increase in conductivity. Exposure to the fuming sulphuric acid blue-shifted the spectrum at the cost of degrading the polymer. Therefore, doping with SO_3 was not found practical in manufacturing a PPV device which could emit a blue light.

Transmission Electron microscopy was employed to investigate crystallinity in PPV. The main objective of this study was to examine PPV

morphology and the nature of crystals present in PPV films. A number of researchers reported that amorphous PPV would have better PL and EL yields. Therefore, a thorough investigation of PPV structure and the main cause leading to the formation of crystals seemed quite appropriate. From the evidence presented here, it was concluded that NaCl played an important role in reducing disorder in PPV films by acting as nucleation sites upon which PPV could nucleate and grow. By eliminating NaCl, PPV films of better quality were prepared and IR spectra of these films converted at various temperatures were compared to those of Son *et al* in Fig. 4.6.a and b. The following observations could be made by careful examination of these two figures.

1) In the films prepared by Son *et al*, the ratio of cis- to trans-content of PPV, which may be taken as the degree of amorphousness, decreased with increasing elimination temperature. In contrast, for the samples prepared by the author, this ratio stayed relatively constant once the elimination temperature exceeded 150 °C.

2) The relative content of cis-PPV converted at 250 °C was lower for the films prepared by Son *et al* than the ones synthesized by the author.

Bearing in mind that full conversion of PPV in vacuum requires higher temperatures (T>300 °C), the two observations made above suggested that the synthesis process put forth by Son *et al.* would not necessarily result in a PPV film with a higher degree of amorphousness. Moreover, the higher quantum yield obtained here also indicates that the devices described here perform better than the ones reported by Son.

As a closing note to this section, it is noteworthy to mention that the PPV films converted by Son at 200 °C have a higher cis-content than the ones prepared by us. The cis/trans ratio of their film at this temperature is almost twice that of our PPV. This signifies that their synthesis process can potentially produce a more amorphous PPV with a higher quantum yield, provided that the complete removal of the elimination products could be achieved at T=200 °C. This, however, can not be achieved in vacuum and therefore, the author speculates that their synthesis process can be optimized by conducting the elimination process in argon rather than in vacuum. This has several advantages; 1) almost complete conversion is possible at lower temperatures and, 2) Elimination at lower temperatures ensures higher cis- to trans-PPV ratio and thus a higher luminescent yield.

The corrosion of the positive electrode (ITO) which resulted in an erratic and unstable device behaviour during measurements was also noted. This problem was traced back to the pH of the polymer solution. Since ITO can be corroded in both acidic and basic environments (especially under an applied electric field), measures were taken accordingly to attain a near neutral solution which did not attack the electrode. This ensured the integrity and continuity of ITO contacts.

Experiments conducted here and elsewhere concluded that full conversion of PPV under vacuum was attained at T>300 °C. Several disadvantages were found with this conversion process. It was shown in Fig. 5.3 that with increasing the elimination temperature the intensity of PL light decreased substantially. Assuming that processes leading to El and PL in PPV are similar and that the EL efficiency is about a quarter of PL efficiency, as indicated by Yan (1994), EL efficiency of PPV would also decrease with increasing the conversion temperature. Thus, argon was used in the conversion process. The conversion of PPV under argon gas proved highly effective. This was illustrated in Fig. 5.6 where PL and UV-visible absorption of an argon-converted PPV film were compared with the vacuum-converted PPV films.

Conversion of PPV was achieved at temperatures as low as 160 °C.

The use of argon further reduced the reaction of the polymer film with oxygen during the elimination process. This was substantiated by employing the impedance analysis technique. The presence of the extra semi-circle on the cole-cole plot of an argon-converted sample representing the interface was not detected. Therefore, it was concluded that the interface layer, arising due to the polymer oxidation, was not formed under argon. This statement, however, has to be examined more carefully. Although PPV diodes made under argon have a lower threshold voltage, are brighter over a larger area, and have a better performance than the vacuum-converted devices, the author does not wish to rule out the possible existence of the interface. The metal/PPV interface may also arises due to the metal oxidation during evaporation coating. Further, it is speculated that if the metal (e.g. Al) does not form any bond with the PPV surface, a physical gap may be created leading to the formation of a space charge and thus an interface. Consequently, this limits the charge injection across the interface, increases the drive voltage and reducing the EL efficiency.

The devices made under argon showed substantial improvement in stability and performance. The threshold voltage for electroluminescence was significantly lowered, and a uniform light was emitted from the entire device. The electroluminescence showed a linear dependence on the input power, which implied that charge injection limited the output light. After passing the linear regime, the EL intensity reached saturation and did not increase significantly with the current density. The reason for EL saturation is not quite clear but it is attempted to provide some explanation as follows. EL saturation may be the direct result of non-radiative e-h recombination. Although at and above saturation, more charged species are injected into the device, the majority of them might pass through the device without forming e-h pairs in the material. In other words, with increasing bias voltage the polymer degrades locally as a result of Joule heating. Material degradation subsequently causes the top and bottom electrodes (ITO and e.g. Al) to form a short circuit which can draw more current without contributing to the EL. Polymer degradation was in fact detected in the form of locally burnt spots on the EL devices by using an optical microscope. These "short spots" are believed to be the cause for increased current density.

The EL efficiency of the best samples measured was about 0.59%. This is relatively higher than the values reported by other investigators for single layer organic devices. The performance of these devices was measured under ambient conditions and the longest lifetime achieved was about 160 hours. Although longer lifetimes have been reported for organic EL devices by other researchers, it is not clear whether their device was encapsulated and/or whether their measurements were carried out under an inert atmosphere.

The EL devices showed a rectifying behaviour and photons were emitted by the recombination of the injected electrons and holes from the negative (Al, or Mg) and positive (ITO) electrodes, respectively. Under a strong electric field (in the order of MV/cm) electrons are injected into the lowest unoccupied molecular orbital (LUMO) and holes are injected into the highest occupied molecular orbital (HOMO) of PPV. They then form bound electron hole pairs which can decay to the ground state. The radiative decay of these excitations is responsible for the observed EL, and the non-radiative component is believed to be the cause for low luminescent yield and poor device performance. The use of metals with lower work functions (e.g. Mg, $\Phi=3.7eV$) reduces the barrier height Φ_b as schematically represented in Fig.

6.1. However, the drastic drop in V_{th} as reported here could not be mainly attributed to the barrier height lowering due to the use of Mg. This is because the barrier height for a Mg/PPV contact is about $\Phi_b=\Phi_{Mg}- \Phi_{ppv}=3.7-2.9=0.8eV$ which is not significantly lower than the one for an Al/PPV contact ($\Phi_b=4.3-2.9=1.4eV$) and, therefore, can not account for the decrease in V_{th} mentioned here. It is strongly believed that the decrease in V_{th} and improvement in the light output are due to the use of argon and (partial exclusion of the interface layer mentioned above.

The formation of strongly correlated e-h pairs (excitons) as the excitation modes was substantiated by using the electric field induced fluorescent quenching technique. It was observed that fluorescent quenching and photoresponse in PPV were strongly field dependent and bound e-h pairs were generated upon photoexcitation. These excitons may then recombine to emit photons (as is the case in PL and EL) or dissociate under applied electric field into free carriers which can then be collected at the electrodes.

The fluorescent quenching calculated by us was lower than the one reported by Bassler *et al.* This was attributed to the experimental uncertainty

regarding thickness measurements. A good agreement was achieved if the dielectric constant and thus the thickness were adjusted accordingly.

6.2 Recommended Future Work

From the discussion presented in this thesis, taking the following steps seems quite appropriate in understanding organic LED's and attempting to enhance their performance.

A) A fundamental study seems to be due in correlating the PL response to the EL response under various conditions of sample preparation. Investigators have reported that EL efficiency is approximately a quarter of the PL efficiency and based on this approximation they have predicted a maximum EL efficiency of 15% (Yan 1994). The basis of this prediction is not clear to the author. Nevertheless, experimental verification of the above correlation is important to the evaluation of PPV as potentially being one of the best conjugated polymer for ELD application.

B) IR and transmission electron microscopies are suggested to be employed to further optimize the synthesis process reported by Son *et al*. From

this study the effect of argon as the elimination medium in increasing the amorphousness and decreasing the elimination products could be better understood.

C) A further analysis of the polymer/metal interface is recommended. Standard quasi-static capacitance-voltage measurements should be performed on the metal/PPV/ITO to study the effect of the atmospheric conditions on the barrier hight and the depletion width. Useful information can be obtained from plots $1/C^2$ versus voltage. This can provide an estimate of charge concentration in the depletion region and the depletion width, thus characterizing and optimizing the metal/PPV interface. This consequently would contribute to the enhancement of EL efficiency.
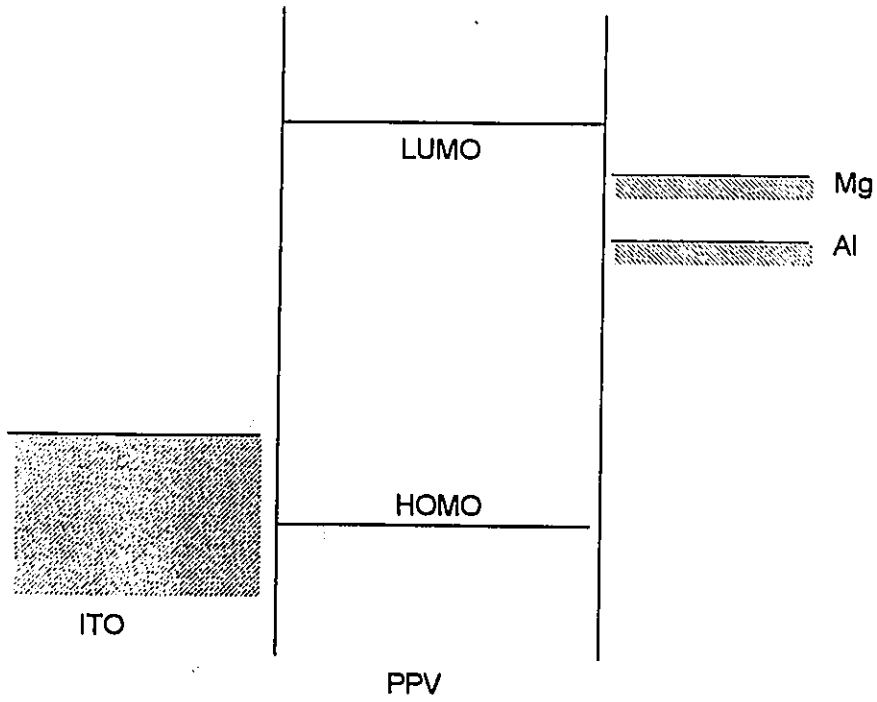
Fig. 6.1. Schematic diagram of the energy profile for a PPV device before contact and at zero bias.

Bibliography

Aldissi M., 1989, *Inherently Conducting Polymers*, Noyes Data Corporation, Park Ridge, New Jersey.

Antoniadis H., Hsieh B.R., Abkowitz M.A., Jenekhe S.A., and Stolka M., 1994, *Syn. Met.*, **62**, p. 265.

Atkins P.W., 1994, *Physical Chemistry*, New York, W.H. Freeman.

Bassler H., Brandl V., Deussen M., Gober E.O., Kersting R., Kurz H., Lemmer U., Mahrt R.F., and Ochse A., 1995, *Pure & Appl. Chem.*, **67** (3), p. 377.

Berggren M., Inganas O., Gustafsson G., Rasmusson J., Andersson M.R., Hjetberg T., and Wennerstrom O., 1994, *Nature*, **372**, p. 444.

Bershtein V.A., and Egorov V.M., 1994, *Differential Scanning Calorimetry of Polymers: Physics, Chemistry, Analysis, Technology*, Ellis Horwood, New York, p. 145.

Bottcher C.J.F., Bordewijk P., 1978, Theory of Electric Polarization, Vol. 2, Elsevier, p. 45.

Bradley D.D.C., 1987-a, *J. Phys. D: Appl. Phys.*, **20**, p. 1389.

Bradley D.D.C., and Friend R.H., 1987-b, *Syn. Met.*, **17**, p. 645.

Braun D. and Heeger A.J., 1991, *Appl. Phys. Lett.*, **58** (18), p. 1982.

Bruce P.G., 1987, in: *Polymer Electrolyte Reviews*, ed. MacCallum J.R., Elsvier Applied Sciences, London/New York, Vol. **1**, p. 237

Burn P.L., Holmes A.B., Kraft A., Bradley D.D.C., Brown A.R., Friend R.H., and Gymer R.W., 1992, *Nature*, **356**, p. 47.

Burroughes J.H., Bradley D.D.C., Brown A.R., Marks R.N., MacKay K., Friend R.H., Burns P.L., and Holmes A.B., 1990, *Nature*, **347**, p. 539.

Capistran J.D., Gagnon D.R., Antoun S., Lenz R.W., and Karasz F.E., 1984, *ACS Polym. Preprints*, **25**, p. 82.

Chiang C.K., Druy M.A., Gau S.C., Heeger A.J., Louis E.J., MacDiarmid A.G., Park Y.W., and Shirakawa H., 1978, *J. American Chem. Soc.*, **100**, p. 1013.

Chiang C.K., Park Y.W., Hegger A.J., Shirakawa H., Louis E.J., and MacDiarmid A.G., 1978, *J. Chem. Phys.*, **69** (11), p. 5098.

Cowie J.M.G., 1991, *Polymers: Chemistry and Physics of Modern Materials*, Aylesbury, London, p. 236 and 417.

Dannetun P., Logdlund M., Fahlman M., Boman M., Stafstrom S., Salaneck W.R., Lazzaroni R., Fredriksson E., Bredas J.L., Graham S., Friend R.H., Holmes A.B., Zambobi R., and Taliani C., 1993, *Syn. Met.*, **55-57**, p. 212.

Dannetun P., Logdlund M., Fredrickson C., Lazzaroni R., Fauquet C., Stafstrom, Spangler C.W., Bredas J.L., and Salaneck W.R., 1994, *J. Chem. Phys.*, **100** (9), P. 6765.

Esteghamatian M., Popovic Z.D., and Xu G., Accepted in April 1996, *J. Phys. Chem.*

Esteghamatian M. and Xu G., 1995, *Syn. Met.* **75**, p. 149.

Esteghamatian M. and Xu G., 1994-a, *Syn. Met.*, **63**, p. 195.

Esteghamatian M. and Xu G., 1994-b, *Appl. Phys. Lett.*, **65** (15), p. 1877.

Fredriksson C., Lazzaroni R., Bredas J.L., Dannetun P., Logdlund M., and Salaneck W.R., 1993, *Syn. Met.*, **55-57**, p. 4632.

Friend R.H., 1992, *Syn. Met.*, **51**, p. 357.

Gagnon D.R., Capistran J.D., Karasz F.E., Lenz R.W., and Antoun S., 1987, *Polym.*, **28**, p. 567.

Gmeiner J., Karg S., Meier M., Riess W., Strohrigel P., Schwoerer M., 1993, *Acta Polym.*, **44**, p. 201.

Greenham N.C., Moratti S.C., Bradley D.D.C., Friend R.H., and Hcmes A.B., 1993, *Nature*, **365**, p. 628.

Heeger A.J., Kivelson S., Schrieffer J.R., and Su W.P., 1988, *Reviews of Modern Physics*, **60** (3), p. 781.

Kido J., Hongawa K., Okujama K., and Ngai K., 1993, *Appl. Phys. Lett.*, **63** (193), p. 2627.

Lee C.H., Yu G., Moses D., and Heeger A.J., 1994, *Phys. Rev. B*, **49** (40), p. 2396.

Lee C.H., Yu G., and Heeger A.J., 1993, *Phys. Rev. B*, **47** (23), p. 15543.

Lide D.R., 1992-1993, *Handbook of Chemistry and Physics*, CRC Press, 73rd Ed.

Marks R.N. and Bradley D.D.C., 1993, *Syn. Met.*, **55-57**, p. 4128.

Murase I., Ohnishi T., Noguchi T., Hirooka M., and Murakami S., 1985, *Mol. Cryst. Liq. Cryst.*, **118**, p. 333.

Ngai K.L. and Rendell R.W., 1986, in: *Handbook of Conducting Polymers*, Vol. II, Ed. Skotheim T.A., Marcel Dekker, NewYork. p. 967.

Naarmann H. and Theophilou N., 1987, *Syn. Met.*, **22**, p. 1.

Pak Y.S., Xu G.,1993-a, *J. Mater. Res.*, **8** (4), p. 923.

Pak Y.S., Xu G., 1993-b, *Solid State Ionics*, **67**, p. 165.

Popovic Z.D., 1983, *J. Chem. Phys.*, **78** (3), p. 1552.

Popovic Z.D., 1984, *Chem. Phys.*, **86**, p. 311.

Popovic Z.D., Loutfi R.O., and Hor A.M., 1985, *Can. J. Chem.*, **63**, p. 134.

Rauscher U., Bassler H., Bradley D.D.C., and Hennecke M., 1990, *Phys. Rev. B*, **42** (16), p. 9830.

Riess W., Karg S., Dyanokov V., Meier M., and Shwoerer M., 1994, *J. Luminescence*, **60-61**, p. 906.

Roth S., 1991, in: *Hopping Transport in Solids,* Eds. Pollak M. and Shklowvskii B., Elsevier Science Publishers, B.V., p. 377.

Shirakawa H., Ito T., and Ikeda S., 1978, *Makromol. Chem.* **179**, p. 1565.

Shirakawa H. and Ikeda S., 1979/1980, *Syn. Met.*, **1**, p. 175.

Son S., Dodabalapur A., Lovinger A.J., and Galvin M.E., 1995, *Sience*, **269**, p. 376.

Tang C.W, Vanslyke S.A., and Chen C.H., 1989, *J. Appl. Phys.*, **65** (9), p. 3610.

Tokito S., Tsutsui T., Tanaka R., and Saito S., 1986, *Jap. J. Appl. Phys.*, **25** (8), p. 680.

Werner A.T., Grem G., Byrne H.J., Leising G., and Roth S., 1995, *Materials Science Forum*, **191**, p. 195.

Wessling R.A., 1986, *J. Polym. Sci.: Polym. Symp.,* **72**, p. 55.

Yan M., Rothberg L.J., Papadimitrakipoulos F., Galvin M.E., and Miller T.M., 1994, *Phys. Rev. Lett.,* **73** (5), p. 744.

Yang Z., Sokolik I., Karasz F.E., 1993, *Macromolecules,* **26**, p.1188.

Young R.J., 1987, *Intro. to Polymers,* Chapman and Hall, London/NewYork p. 158.